AD 410408



TECHNICAL INFORMATION SERIES

# HEAT TRANSFER IN HYPERSONIC FLOW WITH RADIATION AND CHEMICAL REACTION

(4) $8.10 (5) 819 485

# SPACE SCIENCES LABORATORY

AEROPHYSICS SECTION

(6) (7-9)

## HEAT TRANSFER IN HYPERSONIC FLOW WITH RADIATION AND CHEMICAL REACTION*

(12) 76 p. (13) NA (15-19) NA (20) 21

~~By~~

(10) by S. M. Scala and D. H. Sampson.



(14) Rept no. R63SD46

(11) ~~March~~ 1963,

(21) * Presented at the Twenty-First AGARD Combustion and Propulsion Meeting on Supersonic Flow, Chemical Processes and Radiative Transfer, London, England, April 1-5, 1963, under the sponsorship of the Advisory Group for Aeronautical Research and Development, NATO.

MISSILE AND SPACE VEHICLE DEPARTMENT

GENERAL ELECTRIC

# CONTENTS

LIST OF FIGURES

ABSTRACT

During hypervelocity flight, the heat transfer rate to a space vehicle depends on the contributions of aerodynamic (convective, conductive, diffusive and chemically reactive) transport phenomena and radiative transport processes. For certain combinations of vehicle flight speed, altitude, vehicle geometry and planetary gas composition, it is possible for the radiative transport to be of comparable magnitude to, or even to predominate over, the aerodynamic processes, and hence, the twin problems of aerodynamic and radiative heat transfer should be treated self-consistently.

The macroscopic equations for the conservation of mass, momentum and energy (including radiative contributions) are first presented. The hypervelocity flow field is then considered to consist of three definable regions; namely, the shock wave, the influscid flow and boundary layer.

The equations are treated for the optically thin and optically thick limits and numerical results are obtained for the effects of radiation on the structure of the shock wave, and the structure of the boundary layer, including some effects on heat transfer rate to the vehicle.

In order to assess the interplay between radiative energy and chemical energy, the computations of shock wave structure in an optically thin radiating gas are carried out for two limiting cases. In the first model, the chemical kinetic processes are assumed to be initiated after the shock transition, and in the second, the chemical kinetic processes are assumed to be so rapid that the gas is everywhere in a state of dissociation equilibrium.

## 1. INTRODUCTION

The theoretical treatment of radiation in high temperature gases over the full spectral range was put on a sound basis at the turn of the present century with the appearance of Planck's law of radiation, see Ref. (1). A treatment of the general theory of radiative transport has been given in numerous books on astrophysics, Refs. (2) to (4). Methods of solution of the radiative transport equation including the effects of scattering, (scattering is not of much importance in the problems of interest to us here), are given for various conditions in the excellent books by Chandrasekhar, Ref. (5) and Kourganoff, Ref. (6).

Recently, high temperature phenomena have become of increasing interest to engineers and scientists concerned with the problems of hypersonic ballistic re-entry and superorbital entry, into the earth's atmosphere, as well as into the atmospheres of the neighboring planets. It has, therefore, become necessary to adapt the theory developed principally by astrophysicists to the conditions of interest in hypersonic aerospace flight problems, where one of the major differences is the introduction of a solid boundary; namely, the vehicle. We begin by noting that a number of survey articles have recently appeared, which serve to describe the quantitative state of our understanding of hypersonic aerodynamic and radiative heat transfer, see Refs. (7) - (9), and hence, we will restrict our discussion here to conceptual considerations.

The subject of radiative heating in high temperature flowing gases can be classified in terms of the extent of the coupling between the radiative transfer and other energy transport processes, such as the macroscopic motion of the material

particles and the chemical reactions in the gas.

In the earliest theoretical treatments of radiation at hypersonic speeds, (see Figure 1), it was assumed that the shock wave (Region I) could be treated as a discontinuity, and that the viscous boundary layer (Region III) was very thin. Since the equilibrium gas temperatures for suborbital ballistic entry into the earth's atmosphere are usually less than $7000^{\circ}K$, it was also assumed that the inviscid shock layer (Region II) was optically thin, and that the effect of radiative emission on the gas temperature could be neglected. Accordingly, the problem became one of identifying the radiative processes in high temperature air and calculating the frequency and temperature dependence of the absorption coefficients, utilizing experimental data to supplement the theory (e.g., Refs. (10) - (15) ). This same approach has also been recently applied to the prediction of radiative heat transfer at hypersonic speeds in the atmospheres of Mars and Venus, Ref. (16), and at higher gas temperatures during entry into Earth's atmosphere, Refs. (17), (18). The effect of departures from chemical equilibrium on radiative heating has also been treated within the framework of the assumptions of radiative uncoupling, and an optically thin gas layer, Refs. (19) - (21).

Attempts are also being made to consider the coupling between radiative transport and the flow processes; and departures from the assumption of an optically thin gas have been introduced in treating the hypersonic shock layer. Because of the complicated nature of the problem, attention is being given to small disturbance theory, so that the equations may be linearized, (e.g., Refs. (22) - (24) ).

The coupling of radiation and convection has been treated for the one-dimensional case by the Goulards, Ref. (25) for a radiating layer adjacent to a surface.

In their paper, they extend the general equations developed by astrophysicists to include wall effects, but in their calculations make the optically thin approximation.

The coupling between radiation and convection in an inviscid shock layer has been treated by Goulard, Ref. (26) and also by Yoshikawa and Chapman, Ref. (27), using the general equations for a gray gas.

The coupling between radiation and convection in a viscous layer has been treated for the normal shock wave when the gas is optically thick by Sen and Guess, Ref. (28) and by Marshak, Ref. (29). A study of the radiation-resisted shock wave has been carried out by Clarke, Ref. (30).

In view of the experimental data concerning precursor radiation from shocks in air, Ref. (31), attempts are being made to treat the problem analytically. A study of the upstream photoionization produced by a strong shock wave has been carried out recently by Ferrari and Clarke, Ref. (32).

The interaction between radiation and convection in a boundary layer has been treated by Koh and DeSilva, Ref. (33) for the viscous flow over a flat plate, when the gas is assumed to be optically thin. Viskanta and Grosh, Ref. (34) have treated the wedge boundary layer with coupled radiation in the optically thick approximation. However, they evidently did not realize that it is the Rosseland mean absorption coefficient which is appropriate in their case, rather than the Planck mean.

The most recent studies of radiation coupling in the hypersonic boundary layer include the work of Howe, Ref. (35), who considered the injection of an absorbing gas from the surface of the vehicle, and the study of the merged viscous radiating layer by Howe and Viegas, Ref. (36), utilizing the general equations in the gray gas

approximation.

It is also appropriate to mention that theoretical studies of the spectral absorption coefficient of air and air-like species are being carried out without special reference to space vehicle applications, (e.g., Refs. (37), (38) and (39) ).

In the present paper, the authors will consider both shock wave structure and boundary layer structure, for the optically thin and optically thick approximations. As a point of departure, one of the authors has recently re-derived the equations for radiative transport and the coupling between radiation and matter, for quite general conditions, Ref. (40), utilizing a somewhat different point of view than is usually employed in order to clarify the nature of the approximations which go into the usual form of the equations. In this reference, the particular forms of the radiative contribution to the macroscopic equations, which apply for the conditions of interest to aerospace flight, are obtained from the general equations.

## 2. SYMBOLS

| | |
|---|---|
| a, b, c, d | constants |
| $B_\nu(T) = 2h\nu^3/c^2 \left[1 - \exp(h\nu/kT)\right]^{-1}$ | Planck intensity |
| $B(T) = \int_o^\infty B_\nu(T)d\nu = \frac{\sigma}{\pi} T^4$ | |
| c | velocity of light |
| $\overline{C}$ | dimensionless specific heat at constant volume |
| $C_i$ | mass fraction of species i |
| $C_{p_i}$ | specific heat at constant pressure |
| $C_p = \sum_i C_i C_{p_i}$ | frozen specific heat of the gas at constant pressure |
| $C_v = \sum_i C_i C_{v_i}$ | frozen specific heat of the gas at constant volume |
| $\mathcal{D}_{ij}$ | binary diffusion coefficient |
| $D_i^T$ | thermal diffusion coefficient |
| e | internal energy |
| $E_r$ | radiative energy density |
| $E_{r\nu}$ | radiative energy density spectrum |
| $E_i$, $E_j$ | energies of states i and j |
| f | similarity stream function |
| $f_\eta = \frac{u}{u_e}$ | dimensionless tangential velocity |
| $g_i$, $g_j$ | degeneracies of states i and j |

| | |
|---|---|
| $h$ | Planck's constant; static enthalpy of mixture |
| $h_i$ | static enthalpy of species i, including chemical enthalpy |
| $\Delta h^o_{f_i}$ | standard heat of formation of species i evaluated at $T_{ref.}$ |
| $I_\nu(\underset{\rightarrow}{s})$ | specific radiative intensity in direction $\underset{\rightarrow}{s}$ |
| $k$ | frozen thermal conductivity of mixture |
| $\mathcal{k}$ | Boltzmann constant |
| $\overline{K}$ | mean absorption coefficient |
| $K_\nu$ | absorption coefficient |
| $K_p$ | Planck mean absorption coefficient |
| $K_{p_i}$ | equilibrium constant of reaction i |
| $K_R$ | Rosseland mean absorption coefficient |
| $K_T$ | thermal diffusion ratio |
| $L_{ij} = \frac{\rho C_p D_{ij}}{k}$ | frozen Lewis number |
| $\ell = \frac{\rho\mu}{\rho_w \mu_w}$ | dimensionless product of density and viscosity |
| $m$ | integration constant in continuity equation |
| $M_i$ | molecular weight of species i |
| $\overline{M} = \sum_i X_i M_i$ | mean molecular weight of mixture |
| $\underset{\rightarrow}{n}$ | unit vector in the negative y direction |
| $N_a$ | density of absorbers of type "a" |
| $N_i$, $N_j$ | occupation numbers for energy states i and j |
| $p$ | static pressure |

| | |
|---|---|
| $P$ | integration constant in momentum equation |
| $Pr = \frac{C_p \mu}{k}$ | frozen Prandtl number |
| $q$ | radiation path length |
| $Q$ | integration constant in energy equation |
| $\underset{\rightarrow}{Q}$ | heat flux vector |
| $\underset{\rightarrow}{Q}_r$ | radiative energy flux vector |
| $\underset{\rightarrow}{Q}_{r\nu}$ | vector radiative energy flux spectrum |
| $r$ | dimensionless density (shock wave) |
| $\mathcal{R}$ | universal gas constant |
| $R_i$ | gas constant of species i |
| $R_B$ | nose radius of body |
| $\underset{\rightarrow}{s}$ | unit vector in the direction of photon propagation |
| $t$ | time |
| $T$ | temperature |
| $u$ | x component of velocity |
| $v$ | y component of velocity |
| $\underset{\rightarrow}{v}$ | macroscopic stream velocity |
| $V_\infty$ | free stream velocity |
| $\dot{w}_i$ | chemical source term, mass rate of production of species i by chemical reaction per unit volume, per unit time |
| $X_i$ | mole fraction of species i |
| $Y$ | dimensionless distance |
| $Z$ | constant of integration in species equation |

| | |
|---|---|
| $x, y, r_o$ | body-oriented coordinate system |
| $\alpha, \beta$ | constants |
| $\delta$ | thickness of gas layer |
| $\epsilon_w$ | total (hemispherical) emissivity of the wall |
| $\epsilon_{w\nu}$ | spectral emissivity of the wall |
| $\eta, \xi$ | similarity variables |
| $\theta$ | $\cos\theta = \underrightarrow{n} \cdot \underrightarrow{s}$; dimensionless temperature (boundary layer) |
| $\mu$ | viscosity of mixture |
| $\rho$ | density |
| $\sigma$ | Stefan-Boltzmann constant |
| $\bar{\sigma}$ | dimensionless pressure (shock wave) |
| $\sigma_a(\nu)$ | cross section for absorption of photons of frequency $\nu$ by absorbers of type "a" |
| $\tau$ | dimensionless temperature (shock wave) |
| $\upsilon$ | dimensionless velocity (shock wave) |
| $\Omega$ | solid angle |

Subscripts

| | |
|---|---|
| A | atoms |
| e | outer edge of boundary layer |
| i | $i^{th}$ species |
| M | molecules |
| r | radiation |
| s | stagnation point |
| T | thermal |

| | |
|---|---|
| w | wall |
| $-\infty$ | upstream |
| $+\infty$ | downstream |
| $\eta$ | denotes differentiation with respect to $\eta$ |
| $\nu$ | frequency |

Superscripts

| | |
|---|---|
| * | reference state |
| T | thermal |
| - | dimensionless |

## 3. GOVERNING EQUATIONS FOR RADIATING FLOWS

When the approximation of local thermodynamic equilibrium is made and scattering is neglected, the radiative transport equation becomes

$$\frac{\partial I_\nu(\underset{\rightarrow}{s})}{c\,\partial t} + \underset{\rightarrow}{s} \cdot \nabla I_\nu(\underset{\rightarrow}{s}) = K_\nu \left[ B_\nu(T) - I_\nu(\underset{\rightarrow}{s}) \right] . \tag{3.1}$$

In this equation, $K_\nu$ is the absorption coefficient defined by the equation

$$K_\nu = \sum_a N_a \sigma_a(\nu) \left[ 1 - \exp(-h\nu/\mathfrak{k}T) \right] . \tag{3.2}$$

Here, $N_a$ is the number of absorbers of type "a" per unit volume and has the value characteristic of thermal equilibrium at the local matter temperature T, while $\sigma_a(\nu)$ is the cross section for absorption of photons of frequency $\nu$ by these absorbers. The factor $\left[ 1 - \exp(-h\nu/\mathfrak{k}T) \right]$ in Eq. (3.2) has the effect of including induced emission with true absorption. $I_\nu(\underset{\rightarrow}{s})$ is the specific intensity of radiation of frequency $\nu$. The quantity $I_\nu(\underset{\rightarrow}{s})\,d\nu\,d\Omega$ is the amount of radiative energy with frequencies between $\nu$ and $\nu + d\nu$ traveling within the element of solid angle $d\Omega$ about the direction of unit vector $\underset{\rightarrow}{s}$ and crossing unit area perpendicular to $\underset{\rightarrow}{s}$ per unit time. The thermal equilibrium value for $I_\nu(\underset{\rightarrow}{s})$ is the Planck intensity $B_\nu(T)$ given by the equation

$$B_\nu(T) = \frac{2h\nu^3}{c^2} \left[ \exp(h\nu/\mathfrak{k}T) - 1 \right]^{-1} . \tag{3.3}$$

The time derivative term in Eq. (3.1) is negligible unless the tempera-

tures are very high ($kT \sim$ kev.), and there is fairly rapid variation of temperature, density, etc., with time. Thus, in problems of interest here, we can neglect this term and write the radiative transport equation as follows:

$$\underset{\rightarrow}{s} \cdot \nabla I_\nu(\underset{\rightarrow}{s}) = K_\nu \left[ B_\nu(T) - I_\nu(\underset{\rightarrow}{s}) \right]. \tag{3.4}$$

The macroscopic radiative transport equation is obtained by multiplying Eqs. (3.1) or (3.4) by $d\nu d\Omega$ and integrating over $\nu$ and solid angle $\Omega$. The result in the latter case is

$$\nabla \cdot \underset{\rightarrow}{Q}_r = 4\pi \int_0^\infty d\nu K_\nu \left[ B_\nu(T) - c E_{r\nu}/4\pi \right] \tag{3.5}$$

Here, $E_{r\nu} d\nu$ is the energy density of radiation with frequencies between $\nu$ and $\nu + d\nu$, while $\underset{\rightarrow}{Q}_r$ is the total radiative energy flux vector. These are given by the equations

$$E_r = \int_0^\infty E_{r\nu} d\nu; \quad E_{r\nu} = c^{-1} \int_\Omega I_\nu(\underset{\rightarrow}{s}) d\Omega \tag{3.6}$$

and

$$\underset{\rightarrow}{Q}_r = \int_0^\infty \underset{\rightarrow}{Q}_{r\nu} d\nu; \quad \underset{\rightarrow}{Q}_{r\nu} = \int_\Omega \underset{\rightarrow}{s} I_\nu(\underset{\rightarrow}{s}) d\Omega, \tag{3.7}$$

where the integration over $\Omega$ is over all solid angle, i.e., over $4\pi$. For the sake of completeness, we have also included the quantities $\underset{\rightarrow}{Q}_{r\nu}$ (the flux spectrum) and $E_r$ (the total radiative energy density).

The approximation of local thermodynamic equilibrium used in writing

Eqs. (3.1) and (3.4) means that the microscopic matter distribution functions can be approximated by those characteristic of thermal equilibrium at the local temperature T in writing the radiative transport equation. That is, for local thermodynamic equilibrium, the occupations of each pair of energy states are related by a Boltzmann factor as in the case of true thermodynamic equilibrium

$$\frac{N_i}{N_j} = \frac{g_i}{g_j} \exp\left\{-(E_i - E_j)/\kappa T\right\} \tag{3.8}$$

except that now T is a function of position rather than being a constant. In this equation, $N_i$, $E_i$ and $g_i$ are the occupation numbers, energies and degeneracies, respectively, of the state i. Symbols with subscript j refer in a corresponding manner to level j.

The criteria for the validity of the approximation of local thermodynamic equilibrium in the treatment of the radiation is that the interaction of the matter with the radiation, i.e., absorption and emission of photons, gives a small contribution to the right hand side (the collision part) of the Boltzmann equations for the material particles. But, when this is the case, it is also valid to solve the material particle Boltzmann equations with the interaction with the radiation neglected and obtain the usual form for the macroscopic energy transport equation applicable when radiation is unimportant. However, this macroscopic energy transport equation is not correct until either side of Eq. (3.5) is included in the usual expression for the divergence of the energy flux vector. This subject is discussed by one of the authors in much greater detail in Ref. (40).

The approximation of local thermodynamic equilibrium is usually valid;

however, in the case of bound-bound absorption, i.e., molecular band and atomic line absorption, the absorption coefficient is proportional to the matter density $\rho$, while the rate of collisions between material particles is proportional to $\rho^2$. Thus, at very low densities, interaction with the radiation dominates over, or is comparable with, interactions between material particles in determining bound state occupation numbers. In this case, the approximation of local thermodynamic equilibrium breaks down as far as bound state occupation numbers are concerned. When this occurs, the gas is likely to be optically thin because the density is low, which leads to some simplifications.

In the present paper, we always assume local thermodynamic equilibrium to exist except that in some cases the chemical composition is not assumed to be that characteristic of thermodynamic equilibrium. That is, we assume that Eq. (3.8) applies for the relative occupation of the energy levels of a particular species, but the concentration of species is not the thermal equilibrium value. The only effect on the radiation equations is that $N_a$ in Eq. (3.2) should be changed accordingly.

In order to obtain the explicit values for $E_{r\nu}$, $E_r$, $Q_{r\nu}$ and $Q_r$ appearing in Eqs. (3.5) through (3.7) one must solve the radiative transport equation, Eq. (3.4). The general solution to this equation is

$$I_\nu(q) = \int_{q_o}^{q} dq_1 \, K_\nu(q_1) \, B_\nu\left[T(q_1)\right] \exp - \int_{q_1}^{q} K_\nu(q_2)\, dq_2 + I_\nu(q_o) \exp - \int_{q_o}^{q} K_\nu(q_1)\, dq_1 \,, \tag{3.9}$$

where q is the position along the direction $\underset{\rightarrow}{s}$

$$\underset{\rightarrow}{s} \cdot \nabla = \frac{\partial}{\partial q} \tag{3.10}$$

and

$$q_o \leq q_1 \leq q \ . \tag{3.11}$$

$q_o$ is the location along $\underset{\rightarrow}{s}$ of a boundary. The shocked region in front of a blunt object traveling at hypersonic speeds in a planetary atmosphere can be approximated by a plane parallel layer. If y is taken as the preferred direction and we choose unit vector $\underset{\rightarrow}{n}$ to be in the negative y direction, we can make the replacement

$$dq = - dy / \cos\theta \ , \ \cos\theta = \underset{\rightarrow}{s} \cdot \underset{\rightarrow}{n} \ . \tag{3.12}$$

Unless the gas layer is either optically thick or optically thin, Eqs. (3.5), (3.6), (3.7) and (3.9) are difficult to treat numerically even when the gas under consideration can be assumed to be a plane parallel layer and the gray gas approximation, $K_\nu = \overline{K}$ is made. The latter approximation is poor for high temperature air, as is discussed later.

In the present paper we make the assumption that the shocked gas layer is either optically thick, or optically thin. The conditions that must be met for a gas layer of thickness $\delta$, if it is to be optically thick or optically thin are:

$$\int_o^\delta K_\nu (y)\, dy >> 1; \text{ optically thick layer} \tag{3.13}$$

or

$$\int_0^{\delta} K_\nu(y)\, dy << 1; \text{ optically thin layer.} \tag{3.14}$$

First, we consider the optically thick case.

### 3.1 Optically Thick Layer of Gas

When condition (3.13) is satisfied for all important frequencies and the change in temperature within a space interval $K_\nu^{-1}$ is small, one can make a Taylor expansion of $I_\nu(\underset{\rightarrow}{s})$ about $B_\nu(T)$. The result, which is seen by inspection to be a solution of Eq. (3.4) is

$$I_\nu(\underset{\rightarrow}{s}) = B_\nu(T) - \frac{1}{K_\nu}\, \underset{\rightarrow}{s} \cdot \nabla\, B_\nu(T) + \frac{1}{K_\nu}\, \underset{\rightarrow}{s} \cdot \nabla \left[\frac{1}{K_\nu}\, \underset{\rightarrow}{s} \cdot \nabla B_\nu(T)\right] \tag{3.15}$$

$$- \ldots\ldots ; \quad \text{optically thick gas.}$$

For the one-dimensional problem, as seen by Eqs. (3.10) and (3.12),

$$\underset{\rightarrow}{s} \cdot \nabla = -\cos\theta\, d/dy\,. \tag{3.16}$$

With the use of Eqs. (3.6), (3.7) and (3.15) we obtain

$$E_r = \frac{4\pi}{c}\, B(T) = \frac{4\sigma T^4}{c}\,, \quad E_{r\nu} = \frac{4\pi}{c}\, B_\nu(T)\,, \tag{3.17}$$

$$\underset{\rightarrow}{Q}_r = -\frac{4\pi}{3K_R}\, \nabla B(T) = -\frac{16\sigma T^3}{3K_R}\, \nabla T, \quad \underset{\rightarrow}{Q}_{r\nu} = -\frac{4\pi}{3K_\nu}\, \frac{dB_\nu(T)}{dT}\, \nabla T, \tag{3.18}$$

where

$$B(T) = \int_0^\infty B_\nu(T)\, d\nu = \frac{\sigma}{\pi} T^4, \tag{3.19}$$

$$\sigma = \frac{2\pi^4 \hbar^4}{15 c^2 h^3} \quad , \tag{3.20}$$

and $K_R$ is the Rosseland mean absorption coefficient defined by the equation

$$(K_R)^{-1} = \frac{\int_0^\infty \frac{1}{K_\nu} \frac{dB_\nu(T)}{dT}}{\int_0^\infty \frac{dB_\nu(T)}{dT}} \tag{3.21}$$

Thus, in an optically thick gas the radiative contribution to the total energy flux is like a thermal conduction term with a coefficient of conductivity

$$k_{eff} = \frac{16\sigma T^3}{3K_R} \tag{3.22}$$

## 3.2 Optically Thin Layer of Gas

When condition (3.14) is satisfied the exponential factors in Eq. (3.9) can be replaced with unity so that

$$I_\nu(q) = \int_{q_o}^{q} dq_1 \, K_\nu(q_1) \, B_\nu\left[T(q_1)\right] + I_\nu(q_o) \ . \tag{3.23}$$

Condition (3.14) implies that the first term on the right hand side of this equation is negligible relative to $B_\nu(T)$. Thus, if the gas is optically thin for all important fre-

quencies, Eq. (3.5) becomes

$$\nabla \cdot \underset{\sim}{Q}_r = 4\pi \int_0^\infty d\nu K_\nu \left[ B_\nu(T) - \frac{1}{4\pi} \int_\Omega I_\nu(q_o)\, d\Omega \right]. \tag{3.24}$$

$q_o$ is, of course, a function of angle, or $\underset{\rightarrow}{s}$. For the case of a planar wall at temperature $T_w$ on one side of the gas and non-emitting material on the other side, the approximate situation for the shocked region of interest here,

$$\frac{1}{4\pi} \int_\Omega I_\nu(q_o)\, d\Omega \simeq \frac{\epsilon_{w\nu} B_\nu(T_w)}{2} + (1 - \epsilon_{w\nu}) \int_0^\delta K_\nu(y) B_\nu \left[ T(y) \right] dy \tag{3.25}$$

The first term is the contribution due to emission by the wall material and the second term the contribution due to reflection by the wall of radiation emitted by the gas. From condition (3.14) we see that the latter term must always be negligible relative to $K_\nu B_\nu(T)$ and thus cannot contribute significantly to Eq. (3.24). If we assume that the wall emits as a gray body, i.e., $\epsilon_{w\nu} = \epsilon_w$, where $\epsilon_{w\nu}$ and $\epsilon_w$ are the spectral and total hemispherical emissivities of the wall we get

$$\begin{aligned} \nabla \cdot \underset{\sim}{Q}_r &= 4\pi \int_0^\infty d\nu K_\nu \left[ B_\nu(T) - \frac{\epsilon_w}{2} B_\nu(T_w) \right] \\ &= 4\sigma \left[ K_p(T)\, T^4 - \frac{\epsilon_w}{2} K_p(T, T_w)\, T_w^4 \right] , \end{aligned} \tag{3.26}$$

in which $K_p$ is the Planck mean absorption coefficient given by the equation

$$K_p(T) = \int_0^\infty K_\nu B_\nu(T)\, d\nu / B(T) . \tag{3.27}$$

The reason we wrote $K_p(T, T_w)$ in the second term in the final form of the right hand side of Eq. (3.26) is because $K_\nu$ is a function of the gas temperature T, while we integrated over $B_\nu(T_w)$, i.e.,

$$K_p(T, T_w) = \frac{\int_o^\infty K_\nu(T)\, B_\nu(T_w)\, d\nu}{B(T_w)} \tag{3.28}$$

Actually, in the studies carried out in this paper, the wall temperature was chosen to be small enough that the second term on the right hand side of Eq. (3.26) was negligible. When the assumption is made that $\epsilon_{w\nu} = \epsilon_w$ the net flux at the wall in the optically thin case is

$$\begin{aligned} Q_{rw} &= 2\sigma \int_o^\delta K_p T^4 dy - 2(1 - \epsilon_w)\, \sigma \int_o^\delta K_p T^4 dy - \epsilon_w \sigma T_w^4 \\ &= \epsilon_w \left\{ 2\sigma \int_o^\delta K_p T^4 dy - \sigma T_w^4 \right\} \end{aligned} \tag{3.29}$$

In the first form of the right hand side, the first term gives the half of the emission of radiation by the gas which moves toward the wall, the second term accounts for reflection of part of this radiation by the wall, and the third term is the wall emission. Actually as is discussed in Ref. (40) Eqs. (3.25) and (3.29) are not quite correct unless the wall reflectivity and emissivity with respect to intensity $I_\nu(\vec{s})$ are independent of $\vec{s} \cdot \vec{n}$.

Comparing Eqs. (3.21) and (3.27) we see that the mean absorption coefficients $K_R$ and $K_p$ entering the expressions for optically thick and optically thin gases

are different unless $K_\nu$ depends very slightly on $\nu$. For constant $K_\nu$, they are of course equal, otherwise $K_p > K_R$. In the case of an air-like gas, the frequency dependence of $K_\nu$ is sufficiently great that $K_p$ is often one or two orders of magnitude greater than $K_R$, as seen, for example, from the results of Stewart and Pyatt, Ref. (37) for nitrogen. Thus, in the intermediate case when the gas is neither optically thick nor optically thin, it is probably nearly always a very poor approximation to use one single average value for the absorption coefficient for the entire spectrum, (i.e., the gray gas approximation). For example, in using $K = K_p$ in the general equations for the gray gas approximation, if $K_p = 5$, one would approach the optically thick solution for which $K_p$ is inappropriate. On the other hand, for the same conditions of temperature, density, etc., if one used $K = K_R$, which is appropriate in the optically thick limit, the value of $K_R$ would be small, perhaps $\approx 0.1$, then, the general equations for the gray gas approximation would approach the optically thin solution for which $K_R$ is inappropriate. In fact, the variation of $K_\nu$ with frequency is usually large enough, especially at the higher temperatures of interest here, that unless $\int K_p dy$ is very much less than unity or $\int K_R dy$ very much greater than unity, where the integration is over the gas thickness, the gas is likely to be optically thick for some important spectral regions and optically thin for others. Then difficult as this may be, in order to obtain results which are at all accurate, it is probably necessary to devise different appropriate approximation schemes for the differing spectral regions.

### 3.3 The Macroscopic Equations

Following Hirschfelder, Curtiss and Bird, Ref. (41), the governing macroscopic equations for a multicomponent chemically reacting gas may be written

in the following form. The conservation of mass is given by

$$\frac{\partial \rho}{\partial t} + \nabla \cdot (\rho \underset{\rightarrow}{v}) = 0 \quad . \tag{3.30}$$

The conservation of momentum, including the radiation pressure is given by

$$\rho \frac{d\underset{\rightarrow}{v}}{dt} = - \nabla \left(p + \frac{4}{3c}\sigma T^4\right) + \nabla \cdot \underset{\sim}{\tau}_{ij} \tag{3.31}$$

where $\underset{\sim}{\tau}_{ij}$ is the viscous stress tensor. Note that although the radiation pressure is included for completeness, it is actually negligible in the problems of interest here.

Upon neglecting the external forces, the conservation of energy may be written:

$$\rho \frac{de}{dt} = - \nabla \cdot \underset{\rightarrow}{Q} + \underset{\sim}{\pi} : \nabla \underset{\rightarrow}{v} \quad , \tag{3.32}$$

where $\underset{\sim}{\pi}$ is the pressure tensor and

$$\underset{\rightarrow}{Q} = \underset{\rightarrow}{Q}_r - k \nabla T + \sum_i \rho_i \underset{\rightarrow}{V}_i h_i \quad . \tag{3.33}$$

In the optically thick limit, we use Eq. (3.18) to obtain

$$\underset{\rightarrow}{Q} = - \left(k + \frac{16\sigma T^3}{3K_R}\right) \nabla T + \sum_i \rho_i \underset{\rightarrow}{V}_i h_i \quad . \tag{3.34}$$

For the optically thin limit, we make use of Eq. (3.26) (with the second term omitted because the wall temperature we use is sufficiently low) to get

$$\nabla \cdot \underset{\rightarrow}{Q} = - \nabla \cdot (k \nabla T) + 4K_p \sigma T^4 + \nabla \cdot \left(\sum_i \rho_i \underset{\rightarrow}{V}_i h_i\right) \quad . \tag{3.35}$$

Finally, the conservation of chemically reacting species can be written

$$\frac{\partial \rho_i}{\partial t} + \nabla \cdot (\rho_i \underset{\rightarrow}{V}_i) = \dot{w}_i \quad . \tag{3.36}$$

It is appropriate to point out that in writing the equations which are applicable in the optically thick limit, i.e., when the condition given in Eq. (3.13) is satisfied for all important frequencies, we have implicitly assumed that the additional condition

$$\frac{4}{K_\nu T} \left| \nabla T \right| << 1 \tag{3.37}$$

required for the validity of the expansion (3.15) is satisfied. In the special case that the region under consideration consists of the space interval $\Delta y = y_2 - y_1$, between the position $y_1$ at which the temperature $T_1$ is very low, and the position $y_2$ at which the temperature reaches a high value $T_2$, as is usually the situation in a boundary layer or shock wave, either condition (3.13) or (3.37) implies that the other condition holds approximately, as well. This is seen by considering Eq. (3.37)

$$\frac{4}{K_\nu T} \left| \nabla T \right| \approx \frac{4(T_2 - T_1)}{K_\nu T \Delta y} \approx \frac{4}{K_\nu \Delta y} << 1 \tag{3.38}$$

which implies condition (3.13). Whether or not condition (3.37) indeed applies should be tested after the numerical solution for a given situation is obtained. One might expect that it would not apply for the shock wave (Region I) and boundary layer (Region III) which are usually very thin physically. When these regions are not very thin, the gas density is usually quite low, and hence it is expected that they would still be optically thin.

In the optically thin limit, Eq. (3.35) applies if the single condition given by Eq. (3.14) is satisfied for all important frequencies. However, in the latter equation, $\delta$ now represents the total thickness of the shock layer, not just the extent of the boundary layer or the shock wave.

## 4. RADIATION IN A SHOCK WAVE

We begin by noting that one of the authors, Refs. (42), (43) has studied the structure of a normal shock wave, under conditions where the important physico-chemical coupling was the excitation of the internal degrees of freedom including rotational and vibrational modes. The theoretical development presented here follows this earlier work in some features, except that in order to include the radiative phenomena within the framework of a relatively simple model, internal relaxation coupling was not treated at this time.

### 4.1 Optically Thick Shock Wave

Upon utilizing the equations presented in Section 3.3, the governing equations for the one-dimensional steady flow of a viscous, conducting, diffusing, radiating gas are obtained as follows. The conservation of mass is given by:

$$\frac{d}{dy}\ (\rho v) = 0 \tag{4.1}$$

which upon integration becomes:

$$\rho v = m \quad \text{(a constant)} \tag{4.2}$$

The conservation of momentum, neglecting radiation pressure is given by:

$$\rho v\ \frac{du}{dy} = -\frac{dp}{dy} + \frac{d}{dy}\left[\frac{4}{3}\,\mu\,\frac{dv}{dy}\right] \tag{4.3}$$

which upon integration becomes

$$mv + p - \frac{4}{3}\,\mu\,\frac{dv}{dy} = P \quad \text{(a constant)} \tag{4.4}$$

The conservation of species i is given by:

$$\frac{d}{dy}\left(\rho v C_i + j_i\right) = \dot{w}_i \tag{4.5}$$

which when integrated becomes:

$$mC_i + j_i - \Phi_i = Z \quad \text{(a constant)} \tag{4.6}$$

where

$$d\Phi_i = \dot{w}_i dy\ , \tag{4.7}$$

and the one-dimensional diffusion flux vector for a binary mixture may be written, Ref. (44):

$$j_i = -\rho \mathscr{D}_{ij} \left\{ \frac{dC_i}{dy} + \frac{M_i M_j}{\bar{M}^2} \left[ \frac{(\bar{M} - M_i)}{M_i} C_i \frac{d}{dy} \ln p + K_T \frac{d}{dy} \ln T \right] \right\} \tag{4.8}$$

where the thermal diffusion ratio is given by, Ref. (41)

$$K_T = \frac{\rho}{n^2 M_i M_j} \frac{D_i^T}{\mathscr{D}_{ij}} \tag{4.9}$$

For an optically thick gas, the energy equation may be derived utilizing Eqs. (3.32), (3.33) and (3.34):

$$\rho v \frac{dh}{dy} = \frac{d}{dy}\left[ k \left(1 + \frac{16\sigma T^3}{3k K_R}\right) \frac{dT}{dy} \right] - \frac{d}{dy}\left(\sum_i j_i h_i\right) + \frac{4}{3}\mu \left(\frac{dv}{dy}\right)^2 + v \frac{dp}{dy} \tag{4.10}$$

Upon introducing the momentum equation, the definition of the specific heat at constant

volume (assumed constant) and then integrating, we obtain for the conservation of energy in a dissociating diatomic gas:

$$2mC_v T + 2pv + mv^2 - 2k\left(1 + \frac{16\sigma T^3}{3k K_R}\right)\frac{dT}{dy}$$

$$- \frac{8}{3}\mu v \frac{dv}{dy} + 2mC_A\left[\Delta h_{f_A}^{o} - (C_{V_M} - C_{V_A})T\right] \qquad (4.11)$$

$$+ 2j_A\left[(C_{p_A} - C_{p_M})T + \Delta h_{f_A}^{o} + \frac{pK_T}{\rho C_A(1-C_A)}\right] = Q$$

The equation of state is given by:

$$p = \rho R T \qquad (4.12)$$

which may also be written:

$$p = \rho R_M(1 + C_A)T \qquad (4.13)$$

4.2 Optically Thin Shock Wave

For an optically thin shock wave one utilizes Eqs. (4.2), (4.4), (4.6) and (4.13) for the conservation of mass, momentum and chemical species, and the equation of state respectively, but now one utilizes instead the following form of the conservation of energy which is derived from Eqs. (3.32) and (3.35):

$$\rho v \frac{dh}{dy} = \frac{d}{dy}\left(k\frac{dT}{dy}\right) - 4K_p\sigma T^4 - \frac{d}{dy}\left(\sum_i j_i h_i\right) + \frac{4}{3}\mu\left(\frac{dv}{dy}\right)^2 + v\frac{dp}{dy} \qquad (4.14)$$

which can be integrated once to yield:

$$2mC_V T + 2pv + m^2 - 2k\frac{dT}{dy} + 8\sigma\int_o^y K_p T^4 dy$$

$$-\frac{8}{3}\mu v\frac{du}{dy} + 2mC_A\left[\Delta h_{f_A}^o - (C_{V_M} - C_{V_A})T\right] \qquad (4.15)$$

$$+ 2j_A\left[(C_{p_A} - C_{p_M})T + \Delta h_{f_A}^o + \frac{pK_T}{\rho C_A(1 - C_A)}\right] = Q$$

The final set of equations for both the optically thick and optically thin shock wave have been transformed into dimensionless variables in Appendix B.

With regard to the chemistry, we note the following. If one represents the dissociation equilibrium of an air-like molecule by the reaction:

$$M \rightleftharpoons 2A \qquad (4.16)$$

then, the equilibrium constant can be written in terms of the partial pressures of the atoms and molecules, or in terms of the mole fractions.

$$K_{p_A} = \frac{(p_A)^2}{p_M} = \frac{(X_A)^2 p}{X_M} \qquad (4.17)$$

However, since the mass fraction $C_A$ appears explicitly in the governing equations, it is convenient to introduce the relationship between the mole fraction and the mass fraction, and then it can readily be shown that:

$$C_A = \left[\frac{K_{p_A}}{4p + K_{p_A}}\right]^{1/2} \qquad (4.18)$$

In those computations where the gas was assumed to be in dissociation equilibrium, the equilibrium constant utilized was taken as

$$\log_{10} K_{p_A} = 7.00 - \frac{9 \times 10^4}{T\ (^{\circ}R)} \qquad (4.19)$$

which corresponds to the dissociation of nitrogen. The other thermodynamic and transport properties of nitrogen were based on data appearing in Ref. 49 and the dimensionless groups appearing in the equations were calculated in a manner analogous to Refs. 42 and 43.

## 5. RADIATION IN A BOUNDARY LAYER

In this section, we consider the effect of the coupling between the radiation and the viscous flow in the hypersonic laminar boundary layer.

### 5.1 Optically Thick Boundary Layer

Upon utilizing the equations presented in Section 3.3, and introducing the Prandtl boundary layer approximation, one obtains the following governing equations for the hypersonic laminary boundary layer of a viscous, conducting, diffusing, chemically reacting, radiating gas for steady flow over an axi-symmetric body. The conservation of mass is given by:

$$\frac{\partial}{\partial x}(\rho r_o u) + \frac{\partial}{\partial y}(\rho r_o v) = 0 \tag{5.1}$$

The conservation of momentum is:

$$\rho u \frac{\partial u}{\partial x} + \rho v \frac{\partial u}{\partial y} = -\frac{\partial p}{\partial x} + \frac{\partial}{\partial y}\left(\mu \frac{\partial u}{\partial y}\right) \tag{5.2}$$

where it is noted that $\frac{\partial p}{\partial y} = 0$. The conservation of species i, assuming the applicability of Fick's law of diffusion, is given by:

$$\rho u \frac{\partial C_i}{\partial x} + \rho v \frac{\partial C_i}{\partial y} = \frac{\partial}{\partial y}\left[\rho \mathcal{D}_{ij} \frac{\partial C_i}{\partial y} + \frac{D_i^T}{T} \frac{\partial T}{\partial y}\right] + \dot{w}_i \tag{5.3}$$

Finally, utilizing Eqs. (3.32), (3.33) and (3.34) the conservation of energy may be written:

$$\rho C_p \left(u \frac{\partial T}{\partial x} + v \frac{\partial T}{\partial y}\right) = u \frac{\partial p}{\partial x} + \mu \left(\frac{\partial u}{\partial y}\right)^2$$

$$+ \frac{\partial}{\partial y}\left[k\left(1 + \frac{16\sigma T^3}{3k K_R}\right) \frac{\partial T}{\partial y}\right] - \sum_i \dot{w}_i h_i \tag{5.4}$$

$$- \sum_i C_{p_i} M_i \frac{\partial T}{\partial y}\left\{\left[\sum_{j \neq i} \frac{M_j}{M^2} \rho \mathcal{D}_{ij} \frac{\partial X_j}{\partial y}\right] - \frac{D_i^T}{T} \frac{\partial T}{\partial y}\right\}$$

which applies only when the boundary layer is optically thick.

Upon introducing a stream function, the conservation of mass is satisfied identically. That is, $\Psi$ is defined such that

$$\frac{\partial \Psi}{\partial x} = -\rho r_o v \tag{5.5}$$

$$\frac{\partial \Psi}{\partial y} = \rho r_o u \tag{5.6}$$

If we take $\Psi$ in the form

$$\Psi(\xi, \eta) = \sqrt{2\xi}\, f \tag{5.7}$$

and introduce the Mangler-Dorodnitsyn transformation, Refs. (44), (45) and (46):

$$\eta = \frac{\rho_e u_e}{\sqrt{2\xi}} \int_o^y r_o \frac{\rho}{\rho_e}\, dy \tag{5.8}$$

$$\xi = \int_o^x \rho_w \mu_w u_e r_o^2 dx \tag{5.9}$$

the conservation equations are transformed into a set of non-linear ordinary differential equations in the following form: The conservation of momentum becomes

$$(\ell f_{\eta\eta})_\eta + f f_{\eta\eta} + \frac{1}{2}\left[\frac{\rho_e}{\rho} - f_\eta^2\right] = 0 \tag{5.10}$$

The conservation of species takes on the form

$$\left[\frac{\ell}{Pr}\left(Le\, C_{i_\eta} + Le^T \frac{\theta_\eta}{\theta}\right)\right]_\eta + f C_{i_\eta} + \frac{\dot{w}_i}{2\rho\left(\frac{du_e}{dx}\right)} = 0 \tag{5.11}$$

The conservation of energy for an optically thick gas becomes

$$\left[\frac{\bar{C}_p \ell}{Pr}\left(1+\frac{16\sigma T_e^3}{3k K_R}\theta^3\right)\theta_\eta\right]_\eta + \bar{C}_p f \theta_\eta \qquad (5.12)$$

$$- \frac{\sum_i \dot{w}_i h_i}{2\rho T_e \left(\frac{du_e}{dx}\right)} + \frac{\ell}{Pr}\sum_i \left[C_{p_i}\left(L_e C_{i_\eta} + Le^T \frac{\theta_\eta}{\theta}\right)\right]\theta_\eta = 0$$

It is noted that the following definitions were utilized in deriving the preceding equations.

$$\ell = \frac{\rho\mu}{\rho_w \mu_w}\ ;\ Pr = \frac{C_p \mu}{k}\ ;\ \theta = \frac{T}{T_e} \qquad (5.13)$$

$$Le = \frac{\rho C_p \mathcal{D}_{ij}}{k}\ ,\ Le^T = \frac{C_p D_i^T}{k}$$

The boundary conditions to be utilized with Eqs. (5.10), (5.11) and (5.12) are as follows. At the surface, assuming zero slip and no mass transfer:

$$f_{\eta_w} = \frac{u_w}{u_e} = 0 \qquad (5.14)$$

$$f_w = -\frac{r_o \rho_w v_w \sqrt{2\xi}}{\xi_x} = 0 \qquad (5.15)$$

$$\theta_w = \frac{T_w}{T_e} \qquad (5.16)$$

The surface boundary conditions on chemical composition are given, in general, by appropriate chemical kinetic equations. If the gas is assumed to be in equilibrium at the surface, one simply utilizes the appropriate equilibrium constants.

At the outer edge of the boundary layer, one may apply the asymptotic

conditions:

$$\lim_{\eta \to \infty} f_\eta = \lim_{\eta \to \infty} \theta = 1.0 \tag{5.17}$$

and in addition, one sets the following boundary condition on the chemical composition:

$$\lim_{\eta \to \infty} C_i = C_{i_e} \tag{5.18}$$

5.2 Optically Thin Boundary Layer

When the boundary layer is optically thin, one may utilize the equations for the conservation of mass, momentum, and chemical species given by Eqs. (5.10) and (5.11), however, utilizing Eqs. (3.32) and (3.35) the conservation of energy now takes on the form:

$$\rho C_p \left( u \frac{\partial T}{\partial x} + v \frac{\partial T}{\partial y} \right) = u \frac{\partial p}{\partial x} + \mu \left( \frac{\partial u}{\partial y} \right)^2$$

$$+ \frac{\partial}{\partial y} \left( k \frac{\partial T}{\partial y} \right) - 4 K_p \sigma T^4 - \sum_i \dot{w}_i h_i \tag{5.19}$$

$$- \sum_i C_{p_i} M_i \frac{\partial T}{\partial y} \left\{ \left[ \sum_{j \neq i} \frac{M_j}{M^2} \rho \mathcal{D}_{ij} \frac{\partial X_j}{\partial y} \right] - \frac{D_i^T}{T} \frac{\partial T}{\partial y} \right\}$$

which may be transformed into the form:

$$\left( \frac{\bar{C}_p \ell}{Pr} \theta_\eta \right)_\eta + \bar{C}_p f \theta_\eta + \frac{\ell}{Pr} \sum_i \left[ C_{p_i} \left( Le\, C_{i_\eta} + Le^T \frac{\theta_\eta}{\theta} \right) \right] \theta_\eta$$

$$- \frac{\sum_i \dot{w}_i h_i}{2 \rho T_e \left( \frac{du_e}{dx} \right)} - \frac{2 K_p \sigma T_e^3 \theta^4}{\rho \left( \frac{du_e}{dx} \right)} = 0 \tag{5.20}$$

Although the boundary conditions at the surface are the same as those given in Eqs. (5.14), (5.15) and (5.16), the edge boundary conditions are applied somewhat differently in that asymptotic behavior is not necessarily expected. Instead, one has a floating boundary condition, in much the same fashion as the low Reynolds number layer problem, Ref. (47) where an auxilliary integral constraint is introduced. That is, here one may write in first approximation:

$$\theta(\delta) = f_{\eta}(\delta) = 1.0; \quad C_i(\delta) = C_{i_e} \tag{5.21}$$

where $\delta$, the thickness of the radiating viscous layer is not known "a priori" but may be determined by means of additional constraints which are based on the requirement that each variable and its derivatives should match smoothly with the outer shock layer solution.

5.3 Gas Properties

Two different gas models were treated in the numerical computations, constant properties (Figures 12, 13) and variable properties (Figures 14 and 15). For the former, it was assumed that the product of viscosity and density, as well as the mean molecular weight was a constant across the boundary layer; for the latter, these were calculated locally and hence were variable, (see Ref. 49 and TABLE). The Prandtl and Lewis numbers were assumed to be equal to unity in both cases, and for simplicity the thermal conductivity was assumed to be proportional to the square root of the absolute temperature.

## 6. DISCUSSION OF RESULTS

In this section, we will discuss the numerical results obtained during the course of the present investigation. We begin by remarking that the motivation in carrying out the study was to develop additional understanding of radiative transport processes in the hypersonic shock layer. Referring to Figure 1, we observe that the shock layer has been characterized here as consisting of three distinct regions:

Region I - Shock wave

Region II - Influscid* layer

Region III - Boundary layer

Since the equilibration of energy is accomplished throughout the shock layer, the "temperature" has been represented initially by four separate curves representing the translational, rotational, vibrational and electronic excitational modes. After thermal equilibration is complete, of course, the four separate curves merge into a single curve of temperature. It is seen that the normal component of velocity decreases monotonically as the flow approaches the vehicle, and in the absence of ablation or other forms of mass transfer, vanishes identically at the surface. It is also seen that the gas density rises as the flow approaches the surface. Simultaneously with the change in the thermodynamic properties, a change in chemical composition is also taking place. In fact, even before thermal equilibration is necessarily completed, the chemical processes of dissociation and ionization begin. But this clearly

*This word represents the first author's generalization of the word "inviscid" to include the absence of viscous effects, diffusion effects and thermal conduction.

depends on the intermolecular collision frequency and the rates of the various chemical kinetic processes. In general, the problem is extremely complicated since one is dealing with a number of complex physicochemical processes some of which take place in parallel and others in series. Finally, when one introduces the additional complication of radiation, which is in turn related to the gas temperature, the number density of chemically reacting species, and the population of states involved in radiative transitions, the total problem almost appears to be hopeless. Nevertheless, great progress is being made, and in this paper it is expected that additional understanding of coupled radiative phenomena will be added to the existing store of information.

It is now well known that the physical extent of each of these layers is a function of the Reynolds number, Mach number, Knudsen number, surface temperature and vehicle geometry. Thus, at low altitudes, Regions I and III are infinitesimally thick, and Region II envelopes the vehicle, whereas during high altitude flight, the two viscous Regions (I and III) expand, merge and "swallow" Region II. In the present study, we have focussed our attention on Regions I and III, for several reasons, including the fact that these regions are least well understood, and further, where Region II dominates the flow, the existing theoretical models seem quite reasonable.

Figures 2 and 3 show the values used by us for the Rosseland mean absorption coefficient for treating an air-like gas in the optically thick limit. These may be represented analytically by the following expressions for the linearized and quadratic representations:

$$K_R = 4.86 \times 10^{-7} (p)^{1.31} e^{4.56 \times 10^{-4} T} \qquad (6.1)$$

$$K_R = 4.52 \times 10^{-7} (p)^{1.31} e^{(5.18 \times 10^{-4} T - 7.13 \times 10^{-9} T^2)} \qquad (6.2)$$

where the Rosseland mean absorption coefficient $K_R$ is expressed in cm.$^{-1}$, the pressure p in atmospheres, and the temperature T in $^{o}$K. In our computations for an optically thin gas, we used the same functional form for the Planck mean absorption coefficient, but simply assumed that $K_p = 8.3 K_R$.

In Figures 4, 5 and 6 are depicted solutions obtained for the structure of a normal shock wave in an optically thick radiating gas. The range of Mach numbers treated was $12.5 < M < 50$. The symbol $a_1$ denotes the maximum value of the radiation parameter discussed in Appendix A., that is; using symbols of Eq. (A.9):

$$a_1 = \left[\frac{16\sigma T^3}{3k K_R}\right]_{max} \approx \frac{16\sigma}{3\alpha\beta} \frac{1}{\rho_\infty R_m} \left[T^n e^{dT^2 - cT}\right]_{max} \qquad (6.3)$$

In this equation, $K_R$ is given by Eq. (6.1), T is given by Eq. (A.10) and $a_1$ is shown in Figure 19 as a function of P, defined in Eq. (4.4). With $a_1 = 0$, no radiation is present. As $a_1$ is arbitrarily increased, it is seen that radiation broadening occurs on the upstream side of the shock wave. These results are qualitatively similar to those obtained by Sen and Guess, Ref. (28) who treated the low speed range of Mach numbers $1.5 < M < 4$, in that the radiation broadening occurred in the low temperature (upstream) side of the shock wave. However, since their choice of transport and radiative properties, as well as Mach number range, was different (see Appendix A), their quantitative results are, of course, different.

Upon introducing the following definition of the slope thickness in the absence of radiation,

$$(\Delta Y_o) = (\Delta Y)_{a_1 = 0} = \frac{\tau_{+\infty} - \tau_{-\infty}}{\left(\frac{d\tau}{dY}\right)_{max}} \tag{6.4}$$

we obtain a reference value of the nominal shock thickness. In order to calculate the nominal increase in shock wave thickness as a function of Mach number and radiation function $a_1$, the following arbitrary procedure was adopted. First, we write:

$$(\Delta Y)_{a_1} = (Y_2 - Y_1)_{a_1} \tag{6.5}$$

The point $(Y_1)_{a_1 = 0}$ is defined as the point of intersection of the slope $\left[\left(\frac{d\tau}{dY}\right)_{max}\right]_{a_1 = 0}$ and the asymptote $\tau_{-\infty}$. We make a vertical projection from the point $(Y_1)_{a_1 = 0}$ up to the curve $\tau = \left[\tau(Y)\right]_{a_1 = 0}$ which defines a reference temperature at the point $(Y_1)_{a_1 = 0}$. For each solution curve, the point $(Y_1)_{a_1 \neq 0}$ was determined at this reference temperature. Since the results on the downstream side of the shock wave are insensitive to $a_1$, $Y_2$ is defined as the fixed point given by:

$$(Y_2)_{a_1} = (Y_1)_{a_1 = 0} + (\Delta Y)_{a_1 = 0} \tag{6.6}$$

which is also the intersection of the slope $\left[\left(\frac{d\tau}{dY}\right)_{max}\right]_{a_1 = 0}$ with the asymptote $\tau_{+\infty}$.

The ratio $\Delta Y/\Delta Y_o$ is shown in Figure 7, where it is seen that radiation broadening is less pronounced at higher Mach numbers for a given value of $a_1$.

It is noted that in this model of shock wave structure in an optically thick

gas, we have assumed that the gas is characterized by a single temperature; however, it has not been assumed that local thermochemical equilibrium exists, in that the chemical composition was assumed to be frozen at the upstream value. No attempt was made to include chemical kinetics, and thus, the results would tend to apply to the initial part of a shock layer which is optically thick. In order to be self-consistent, we should have used the absorption coefficient corresponding to this frozen chemical composition, (e.g., in air, corresponding to the molecular bands of $N_2$ and $O_2$), rather than that corresponding to complete thermochemical equilibrium (approximately given in Figures 2 and 3). However, estimates indicated that the difference between the two was not too large for most of the conditions of interest here. Thus, in this parametric study, we used the values of $K_R$ given in Figure 2.

The numerical results obtained for the other extreme limiting case of shock wave structure, in an optically thin radiating gas, are shown in Figures 8 through 11. Two values of the Mach number, M = 25 and 35 were treated. Now, as noted, in an optically thin layer, the photon mean free path is large compared with the thickness of the layer, and hence, one may assume that the gas emits but does not absorb radiative energy. Consequently, unlike the optically thick shock wave where the radiative effects appear on the upstream (low temperature) side, here, the radiative effects appear primarily on the downstream (high temperature) side of the shock wave. That is, the high temperature region of the gas radiates in both the upstream and downstream directions, but since energy escapes from the structure of the shock wave, the peak temperature which is reached is lower than would have been obtained if radiation effects were absent.

In this part of the study, the symbol $a_2$ was introduced as a measure of the magnitude of the radiative term appearing in the equation for the conservation of energy in an optically thin shock wave (see Section 4). Thus, the case $a_2 = 0$ corresponds to zero radiation, while the effects of radiation are enhanced as $a_2$ is increased. Examination of Figure 8 shows that as $a_2$ is increased, two things happen; one is that the peak temperature is decreased, but moreover, the downstream conditions are not fixed constants determined "a priori" from the Rankine-Hugoniot conditions. Further, the downstream conditions are not necessarily approached asymptotically, but the temperature continues to decay with increasing distance. That is, since the high temperature gas is continually radiating energy away as it flows, the temperature continues to drop, and the solution must be matched to that obtained in Region II. Of course, if Region II does not exist, due to the viscous merging of Regions I and III, a matching procedure must be utilized at the interface between the contiguous layers.

When the effects of dissociation equilibrium are included, the chemical energy required for dissociation acts to decrease the temperature throughout the shock wave. Hence, the radiative transport, whose temperature dependence appears explictly as $T^4$ and implicitly through $K_p = K_p(T, p)$, is much less important. Consequently, at a Mach number of 25, and for the same values of $a_2$ as utilized in the non-dissociating model, i.e., $0 \leq a_2 \leq 10$, it is seen (see Figure 9) that there are no significant coupled radiative effects for $a_2 \leq 10$.

On the other hand, at the higher Mach number (M = 35), even when dissociation equilibrium was included in the model, (see Figures 10 and 11), radiative coupling was significant for a value of $a_2 = 10$. The specific equation for $a_2$ is:

$$a_2 = \frac{33.2\beta P^{8.31}\sigma\mu^*}{m^9 R_m^{4.5}\sqrt{T^*}} \qquad (6.7)$$

where the symbols are introduced in Appendices A and B. It was found that the solution was relatively insensitive to the effect of pressure on dissociation and hence the error resulting from the fact that a particular choice of $a_2$ also specifies a pressure is small.

Here again, it is noted that a simplified model of the chemistry was utilized in order to obtain qualitative results in a simple manner. Thus, since it was arbitrarily assumed that the dissociation process was rapid, and the ionization process was very slow, the results are applicable to the initial portion of an optically thin shock wave. Since the ionization process also acts to reduce the gas temperature by absorbing the available energy, the radiative coupling might not actually be as pronounced as shown in Figures 10 and 11. It should perhaps also be mentioned that as in the case of the optically thick shock, and as done in the treatment of the boundary layer as well, we used the functional form of the absorption coefficient corresponding to local thermochemical equilibrium. That is, we did not take into account the effect of departures from chemical equilibrium on the functional form of $K_p$ and $K_R$.

In Figures 12 through 16 are presented the numerical results of an investigation of the optically thick boundary layer, (Region III), for two values of the boundary layer edge temperature, $T_e = 20,000^{\circ}R$ and $40,000^{\circ}R$. The wall temperature was arbitrarily taken equal to $4,000^{\circ}R$ and the computations were carried out for the case of constant properties and variable properties. Curves of the variation of tangential velocity u and gas temperature T, normalized by their edge values, are shown as a function of $\eta$, the stretched y coordinate. In this part of the study, the symbol $a_3$ denotes the

maximum value of the radiation parameter, which therefore plays the same role as $a_1$, where $a_3$ is given by Eq. (A.4) and T is obtained from Eqs. (A.6) and (A.7). The dependence of $a_3$ upon $p_e$ is shown in Figure 19 for both the linear and quadratic forms of $K_R$.

Here again, it is seen that radiation broadening occurs as $a_3$ is increased. However, as shown in Figure 16, thickening of the layer is not the only effect. Upon making a plot of the ratio of the sum of the conductive and radiative terms normalized by the conductive term, where the numerical solutions were obtained by keeping the boundary conditions fixed and merely changing $a_3$, one finds that this ratio increases linearly with $a_3$, and at a rather substantial rate.

In Figures 17 and 18, we have shown a typical set of numerical results obtained for an optically thin boundary layer. The variation of the dimensionless tangential velocity and gas temperature is shown as a function of the variable $\eta$, for three different values of the radiation parameter $a_4$. Here it is noted that $a_4$ is given by:

$$a_4 = \frac{2(K_p)_{T_e} \sigma T_e^3}{\rho\theta \frac{du_e}{dx}} \tag{6.9}$$

which may be simplified by introducing the hypersonic approximation

$$\frac{du_e}{dx} = \frac{1}{R_B}\sqrt{2\bar{R}_e T_e} \tag{6.10}$$

so that we also obtain:

$$a_4 \approx \frac{\sqrt{2}(K_p)_{T_e} \sigma T_e^{2.5} R_B}{\rho_e \sqrt{\bar{R}_e}} \tag{6.11}$$

Which one of the solutions given in Figures 17 and 18 applies in a given physical situation would depend on matching this solution smoothly into the solution to the

outer contiguous layer.

The condition, Eq. (3.14), for the shock layer to be optically thin can always be reached for sufficiently small values of the vehicle nose radius $R_B$. The values pertaining to our choices for $a_2$ and $a_4$, given by Eqs. (6.7) and (6.11) are, for the most part, physically reasonable. On the other hand, the pressures corresponding to the choices for $a_1$ and $a_3$ are seen from Figure 19 to be extremely large, $p \sim 10^5$ to $10^6$ atmospheres. Moreover, condition (3.37) (which as noted in Section 3 implies that condition (3.13) applies as well for the shock wave or boundary layer) is found by inspection of our results not to be satisfied when $K_R$ is introduced for $K_\nu$. This indicates that the shock wave and boundary layer are not optically thick. In fact, the total shock layer is usually more nearly optically thin than thick. However, upon introducing the hypersonic approximation that the total shock layer thickness is of the order of $0.1\ R_B$, we see from Figure 3 that condition (3.13) can be approximately satisfied for the total shock layer for realistic values of the stagnation pressure and large values of $R_B$, such as may be expected for manned space vehicles. If the total shock layer is optically thick and the gas temperatures large enough for radiation to dominate over aerodynamic transport processes, one would expect the boundary layer and shock wave to adjust themselves such that they would each be of the order of a photon mean free path in thickness, i.e.,

$$\int_0^\delta \overline{K}\, dy \sim 1 \qquad (6.12)$$

where $\delta$ is the thickness of the shock wave or boundary layer and $\overline{K}$ an average of $K_\nu$ over $\nu$. The reason for expecting this self-adjustment in the thickness is that if the shock wave and boundary layer were thin while the total layer is thick, black body radiation

flux would flow out each side of the shock layer. If the temperature is high, the heat content of the shock layer would not be great enough to sustain this and the shock wave and boundary layer would broaden out to the extent that a significant portion of the radiative flux from Region II would be reabsorbed.

## 7. CONCLUSIONS

In this paper, which gives an introductory treatment of the coupling between radiative transport processes and hypersonic chemically reacting flows, four different problems have been investigated, i.e. the hypersonic shock wave structure problem and the hypersonic laminar boundary layer problem, for both the optically thin and optically thick limits.

The true physical situation will lie between these limits, and usually much closer to the optically thin limit, however, by treating the problem in the two limits, it is felt that certain features of the true solution have been captured. For example, in the case of shock wave structure, it is anticipated that the peak shock temperature will be diminished by radiation, since some of the radiation escapes without being reabsorbed. On the other hand, some of the radiation is absorbed, and hence, the shock wave will be broadened on the upstream side.

## 8. ACKNOWLEDGMENTS

The authors wish to express their appreciation to Mr. J. P. Young who obtained the numerical solutions on the Electronic Associates EA231R electronic analog computer, to Messers. John Wilson and Charles Cook for their assistance in the numerical computations and preparation of the graphs, and to Miss Joanne Zinchak for typing the manuscript.

This study was supported by the General Electric Company through its Contractors' Independent Research Program.

## 9. REFERENCES


1. Planck, M., The Theory of Heat Radiation, Dover Publications, 1959, (Translation of Waermestrahlung, 1913).
2. Rosseland, S., Theoretical Astrophysics, Oxford University Press, 1936.
3. Chandrasekhar, S., An Introduction to the Study of Stellar Structure, University of Chicago Press, 1939.
4. Unsöld, A., Physik der Sternatmosphären, Julius Springer, Berlin 1955.
5. Chandrasekhar, S., Radiative Transfer, Oxford University Press, 1950.
6. Kourganoff, V., Basic Methods in Transfer Problems, Clarendon Press, Oxford, 1952.
7. Allen, H. J., "Gas Dynamics Problems of Space Vehicles", NASA SP-24, November 1962, pp. 1 - 17.
8. Scala, S. M., "The Hypersonic Environment, Heat Transfer in Multicomponent Gases, Aerospace Engineering, High Temperatures Issue, Vol. 22, No. 1, January 1963, pp. 10 - 22.
9. Cheng, H. K., "Recent Advances in Hypersonic Flow Research", AIAA Journal, Vol. 1, No. 2, February 1963, pp. 295 - 310.
10. Wurster, W. H., Glick, H. S., and Treanor, C. E., "Radiative Properties of High Temperature Air", Cornell Aero. Lab. Rept. QM 997-A1, Sept. 1957.
11. Kivel, B. and Bailey, K., "Tables of Radiation from High Temperature Air", Report 21, AVCO Everett Research Lab., December 1957.
12. Meyerott, R. E., "Radiation Heat Transfer to Hypersonic Vehicles: in Combustion and Propulsion, Third AGARD Colloquium, Pergamon Press, 1958, pp. 431 - 447.

13. Meyerott, R. E., Sokoloff, J. and Nicholls, R. W., "Absorption Coefficients of Air", LMSD 288052, Lockheed Aircraft Corp., July 1960.

14. Breene, R. G., Jr., and Nardone, M. C., "Radiant Emission from High Temperature Air", General Electric Co., MSVD, TIS R61SD020, May 1961.

15. Treanor, C. E., "Radiation at Hypersonic Speeds", in Hypersonic Flow Research (F. R. Riddell, Ed.), Academic Press, New York, 1962.

16. Breene, R. G., Jr., and Nardone, M. C., "Radiation in the Atmospheres of the Terrestrial Planets", in Dynamics of Manned Planetary Entry (Scala, Harrison and Rogers, Eds.) John Wiley and Sons, Inc., New York, 1963.

17. Yoshikawa, K. K., and Wick, B. H., "Radiative Heat Transfer During Atmospheric Entry at Parabolic Velocity," NASA TN D-1074, 1961.

18. Breene, R. G., Jr., Nardone, M. C., Riethof, T. R., and Zeldin, S., "Radiance of Species in High Temperature Air," General Electric Co., MSVD, TIS R62SD52, July 1962.

19. Camm, J. C., Kivel, B., Taylor, R. L., and Teare, J. D., "Absolute Intensity of Non-equilibrium Radiation in Air and Stagnation Heating at High Altitudes", J. Quant. Spectroscopy and Rad. Trans., Vol. 1, No. 1, Sept. 1961, pp. 53 - 75.

20. Teare, J. D., Georgiev, S. and Allen, R. A., "Radiation from the Non-equilibrium Shock Front" in Hypersonic Flow Research, (F. R. Riddell, Ed.), Academic Press, New York, 1962, pp. 281 - 317.

21. Allen, R. A., Rose, P. H., and Camm, J. C., "Non-equilibrium and Equilibrium Radiation at Super-satellite Re-entry Velocities", IAS Paper 63 - 77, January 1963.

22. Prokof'ev, V. A., "Propagation of Forced Plane Compression Waves of Small Amplitude in a Viscous Gas when Radiation is taken into Account", ARS Journal, Vol. 31, No. 7, July 1961, pp. 988.

23. Baldwin, B. S., Jr., "The Propagation of Plane Acoustic Waves in a Radiating Gas", NASA TR R-138, 1962.

24. Vincenti, W. G. and Baldwin, B. S., Jr., "Effects of Thermal Radiation on the Propagation of Plane Acoustic Waves", Jour. Fluid Mechanics, Vol. 12, Part 3, March 1962 pp. 449 - 477.

25. Goulard, R. and Goulard, M., "One-Dimensional Energy Transfer in Radiant Media", Int'l. Jour. Heat and Mass Transfer, Vol. 1, No. 1, 1960, pp. 81 - 91.

26. Goulard, R., "The Coupling of Radiation and Convection in Detached Shock Layers", Bendix Products Div., Applied Sciences Lab., April 1959.

27. Yoshikawa, K. Y. and Chapman, D. R., "Radiative Heat Transfer and Absorption Behind a Hypersonic Normal Shock Wave", NASA TN D-1424, September 1962.

28. Sen, H. K., and Guess, A. W., "Radiation Effects in Shock-Wave Structure", Phys. Rev., Vol. 108, No. 3, November 1957, pp. 560 - 564.

29. Marshak, R. E., "Effect of Radiation on Shock Wave Structure", Phys. Fluids, Vol. 1, No. 1, January 1958, pp. 24 - 29.

30. Clarke, J. F., "Radiation-Resisted Shock Waves", Phys. Fluids, Vol. 5, No. 11, November 1962, pp. 1347 - 1361.

31. Hammerling, P., "Ionization Effects of Precursor Radiation from Shocks in Air", AVCO Research Lab Report 98, 1960.

32. Ferrari, C. and Clarke, J. H., "Photoionization Upstream of a Strong Shock Wave", Report CM-1020, Brown University, January 1963. Also to be published in AGARD proceedings.

33. Koh, J. C. Y., and DeSilva, C. N., "Interaction Between Radiation and Convection in the Hypersonic Boundary Layer on a Flat Plate", ARS Preprint 2205 - 61, October 9, 1961.

34. Viskanta, R., and Grosh, R. J., "Boundary Layer in Thermal Radiation Absorbing and Emitting Media", International Journal of Heat and Mass Transfer, Vol. 5, September 1962, pp. 795 - 806.

35. Howe, J. T., "Shielding of Partially Reflecting Stagnation Region Surfaces Against Radiation by Transpiration of an Absorbing Gas", NASA TR R-95, 1961.

36. Howe, J. T., and Viegas, J. R., "Solutions of the Ionized Radiating Shock Layer, Including Reabsorption and Foreign Species Effects, and Stagnation Region Heat Transfer", NASA TR R-159, 1963.

37. Stewart, J. C. and Pyatt, K. D., Jr., "Theoretical Study of Optical Properties, Research Directorate, AFSWC, AFSC, Report AFSWC TR 61-71, Vols. I, II and III September 1961.

38. Armstrong, B. H., Sokoloff, J., Nicholls, R. W., Holland, D. H. and Meyerott, R. E., Radiative Properties of High Temperature Air, J. Quant. Spectroscopy and Rad. Trans. Vol. 1, No. 2, November 1961, pp. 143.

39. Churchill, D. R., Hagstrom, S. A., Weisner, J. D., and Armstrong, B. H., "The Spectral Absorption Coefficient of Heated Air," Lockheed M. S. C. Report 2-57-62-2, November 1962.

40. Sampson, D. H., "Radiative Contributions to Energy and Momentum Transport in a Gas", General Electric Co., M. S. D. TIS R63SD14, March, 1963.

41. Hirschfelder, J. O., Curtiss, C. F. and Bird, R. B., Molecular Theory of Gases and Liquids, John Wiley and Sons, 1954.

42. Talbot, L., and Scala, S. M., "Shock Wave Structure in a Relaxing Diatomic Gas", Proceedings of the Second International Symposium on Rarefied Gas Dynamics, (L. Talbot, Ed.), Academic Press, 1961, pp. 603 - 622.

43. Scala, S. M. and Talbot, L., "Shock Wave Structure with Rotational and Vibrational Relaxation", Proceedings of the Third International Symposium on Rarefied Gas Dynamics, (J. Laurmann, Ed.), Academic Press, 1963.

44. Lees, L., "Laminar Heat Transfer Over Blunt Bodies at Hypersonic Flight Speeds", Jet Propulsion, Vol. 26, No. 4, 1956, pp. 259-269.

45. Fay, J. and Riddell, F., "Theory of Stagnation Point Heat Transfer in Dissociated Air", J. Aero. Sci., Vol. 25, No. 2, 1958, pp. 78-85.

46. Scala, S. M. and Baulknight, C. W., "Transport and Thermodynamic Properties in a Hypersonic Laminar Boundary Layer, Part II - Applications", ARS Journal, Vol. 30, No. 4, 1960, pp. 329-336.

47. Goldberg, L. and Scala, S. M., "Mass Transfer in the Hypersonic Low Reynolds Number Viscous Layer", IAS Preprint No. 62-80, January 1962.

48. Grad, H., "The Profile of a Steady State Plane Shock Wave", Communications Pure and Applied Math., Vol. V, 1952, pp. 257-300.

49. Scala, S. M. and Baulknight, C. W., "Transport and Thermodynamic Properties in a Hypersonic Boundary Layer, Part I - Properties of the Pure Species", ARS Journal, Vol. 29, No. 1, 1959, pp. 39-45.

TABLE - GAS PROPERTIES

$$\overline{C}_p = 0.3 \ \frac{BTU}{lb\ {}^oR}$$

$$h_N = 1.43 \times 10^4 + 0.35\ T({}^oR), \ \frac{BTU}{lb}$$

$$h_{N_2} = -280 + 0.32\ T({}^oR), \ \frac{BTU}{lb}$$

$$k = 2.79 \times 10^{-5} \sqrt{T({}^oR)}\ , \ \frac{watts}{cm\ {}^oK}$$

$$\sigma = 5.67 \times 10^{-12} \ \frac{watts}{cm^2\ {}^oK^4}$$

$$\mu = 1.16 \times 10^{-5} \left(\frac{717}{225 + T({}^oR)}\right) \left(\frac{T({}^oR)}{492}\right)^{3/2}, \ \frac{lb}{ft.\ sec.}$$

Note that k was utilized in the calculation of the radiation parameter and that $\mu$ was utilized in calculating $\ell$, but not in the calculation of the Prandtl number which was assumed to be equal to unity.

## APPENDIX A - COMPARISON OF RADIATION AND CONDUCTION TERMS IN AN OPTICALLY THICK GAS

For an optically thick gas, we may write the energy flux vector in the form:

$$\underset{\sim}{Q} = -k\left(1 + \frac{16\,\sigma T^3}{3k\,K_R}\right)\nabla T + \sum_i \rho_i \underset{\rightarrow}{V}_i h_i \qquad \text{(A. 1)}$$

In order to assess the relative importance of the radiative and conductive contributions in both a boundary layer and a shock wave, we must compare the magnitude of the dimensionless radiative function $16\,\sigma\,T^3/3kK_R$ with unity. Since the former is not a constant, the comparison should be made at that value of the temperature at which the radiative function is a maximum.

Let us therefore introduce the following functional forms:

$$k = \alpha\,T^a \qquad \text{(A. 2)}$$

and

$$K_R = \beta\,p^b\,e^{cT - dT^2} \qquad \text{(A. 3)}$$

where $\alpha$, $\beta$, a, b, c and d are constants. Then, there follows:

$$\frac{16\,\sigma T^3}{3kK_R} = \left[\frac{16\sigma}{3\alpha\beta\,p^b}\right] T^m\,e^{dT^2 - CT} \qquad \text{(A. 4)}$$

where $m = 3 - a$. If $c >> d$, the radiative function will be a maximum at the lower gas temperatures which appear in the problem, and will decrease as the temperature rises. In general, however, the radiation function will not have a monotonic behavior,

and therefore we are interested in determining the temperature at which a maximum is attained.

In a boundary layer, the local pressure is a constant, hence upon setting the partial derivative of Eq. (A. 4) with respect to temperature, at constant pressure, equal to zero, we obtain the quadratic equation

$$2dT^2 - cT + m = 0 \tag{A.5}$$

and hence the radiative function is stationary when the temperature is given by

$$T = m/c \; ; \quad (d = 0) \tag{A.6}$$

$$T = \frac{c \pm \sqrt{c^2 - 8dm}}{4d} \; ; \quad (d \neq 0) \tag{A.7}$$

If $m > 0$, and $c^2 > 8\,dm$, where a, b, c and d are positive constants, it is seen that the radiation function goes through a maximum when one utilizes the minus sign (low gas temperatures) and goes through a minimum when one selects the plus sign (high gas temperatures).

In the case of the shock wave structure problem, we note that the flow is one-dimensional, and moreover, the pressure is not constant through the layer. Hence we may introduce the equation of state and the conservation of mass to obtain

$$p^b = (\rho \bar{R} T)^b = \left(\frac{\rho_\infty V_\infty \bar{R} T}{v}\right)^b \tag{A.8}$$

in which case the radiation function becomes:

$$\frac{16\sigma T^3}{3kK_R} = \left[\left(\frac{16\sigma}{3\alpha\beta}\right)\left(\frac{v}{\rho_\infty V_\infty \bar{R}}\right)^b\right] T^n e^{dT^2 - cT} \tag{A.9}$$

where $n = 3 - a - b$. If one assumes that both $\overline{R}$ and v are changing slowly in the low temperature regime, then the radiative function is a maximum when

$$T \approx n/c; \quad d = 0 \tag{A.10}$$

$$T \approx \frac{\sqrt{c - c^2 - 8\,dn}}{4d} \quad ; \quad (d \neq 0) \tag{A.11}$$

Thus, upon substituting either Eq. (A.6) or (A.7) into Eq. (A.4), or either Eq. (A. 10) or (A.11) into Eq. (A.9), respectively one can immediately determine, "a priori", the relative importance of the radiation and conduction terms. It should be noted that if the radiative function is a sharply peaked function of temperature, then, of course, the average value of the radiative function can be considerably smaller than its maximum value.

It is also noted that if we had selected, for example, the functional forms for thermal conductivity and absorption coefficient utilized by Sen and Guess (Ref. 28) i.e.

$$k = \alpha T^{2.5} \tag{A.12}$$

$$K_R = \beta P T^{-3.5} \tag{A.13}$$

then the radiative function would increase monotonically very nearly as $T^3$ and the major contribution of the radiation would appear at the highest temperatures encountered in a given physical problem.

## APPENDIX B - NORMALIZATION OF THE SHOCK WAVE EQUATIONS

We will derive here the non-dimensional form of the equations. Following Grad's notation, Ref. (48), we introduce the following dimensionless variables

$$\upsilon = \frac{mv}{P}\ ;\ r = \frac{P\rho}{m^2}$$

$$\tau = \frac{m^2 R_m T}{p^2}\ ;\ \bar{\sigma} = \frac{p}{P} \qquad \text{(B-1)}$$

$$\bar{\alpha} = \frac{mQ}{p^2}$$

Upon defining the transport lengths,

$$L_\mu = \frac{\mu}{m};\ L_t = \frac{k}{mR_m} \qquad \text{(B-2)}$$

and putting the transport properties in the form

$$\mu = C_1 T^{1/2}$$

$$\mathcal{D}_{AM} = C_2 T^{3/2}/p \qquad \text{(B-3)}$$

$$k = C_3 T^{1/2}$$

We can select a reference temperature $T^*$ and introduce the non-dimensional spatial variable

$$Y = \frac{\tau^{*1/2} y}{L_\mu^*} \qquad \text{(B-4)}$$

where

$$\tau^* = \frac{m^2 R_m T^*}{p^2} \tag{B-5}$$

and

$$L_\mu^* = \frac{\mu^*}{m} \tag{B-6}$$

The following equations are then obtained in terms of the non-dimensional variables.

The conservation of mass is:

$$r\upsilon = 1.0 \tag{B-7}$$

The conservation of momentum is:

$$\frac{4}{3}\tau^{1/2}\upsilon\frac{d\upsilon}{dY} = \upsilon^2 + \tau(1 + C_A) - \upsilon \tag{B-8}$$

The conservation of species is:

$$j_A = \Phi_A - m\,(C_A - C_{A_{-\infty}}) \tag{B-9}$$

where the diffusion flux is:

$$j_A = -\,m\theta_D^{1/2}\left[\frac{1}{1 + C_A}\frac{dC_A}{dY} + \frac{C_A(1 - C_A)}{2}\frac{1}{\bar{\sigma}}\frac{d\bar{\sigma}}{dY} + \frac{1 + C_A}{2}\frac{K_T}{\tau}\frac{d\tau}{dY}\right] \tag{B-10}$$

and the chemical source term is:

$$\Phi_A = \int \dot{w}_A \frac{L_\mu^*}{\tau^{*1/2}}\,dY \tag{B-11}$$

For an optically thick gas, the conservation of energy is given by:

$$\theta_t \left[1 + \frac{16\sigma T^3}{3kK_R}\right] \tau^{1/2} \frac{d\tau}{dY} = \frac{j_A}{m}\left[\left(\bar{C}_A - \bar{C}_m\right)\tau + \Delta H + \frac{k_T(1+C_A)}{C_A(1-C_A)}\tau\right]$$

$$+ C_A\left[\left(\bar{C}_A - \bar{C}_m\right)\tau + \Delta H\right] + \bar{C}_m\tau + \upsilon - \frac{\upsilon^2}{2} - \frac{\bar{\alpha}}{2} \qquad \text{(B-12)}$$

In the above equations:

$$\Delta H = \frac{m^2}{P^2}\Delta h_{f_A}{}^o$$

$$\bar{C}_A = \frac{C_{v_A}}{R_m} \quad ; \quad \bar{C}_m = \frac{C_{v_m}}{R_m} \qquad \text{(B-13)}$$

and the dimensionless ratios are

$$\theta_t = \frac{L_t^*}{L_\mu^*} \quad ; \quad \theta_{\mathcal{D}} = \frac{L_{\mathcal{D}}^*}{L_\mu^*}\,\bar{\sigma}^* \qquad \text{(B-14)}$$

where $\theta_t$ has the behavior of the reciprocal of the Prandtl number and $\theta_{\mathcal{D}}$ has the behavior of the reciprocal of the Schmidt number.

In addition one has the equation of state for a dissociating diatomic gas

$$\bar{\sigma} = r(1 + C_A)\tau \qquad \text{(B-15)}$$

For an optically thin radiating gas, equation (B-12) is replaced by:

$$\theta_t \tau^{1/2} \frac{d\tau}{dY} = \frac{j_A}{m}\left[\left(\bar{C}_A - \bar{C}_m\right)\tau + \Delta H + \frac{k_T(1+C_A)}{C_A(1-C_A)}\tau\right] + \bar{C}_m\tau + \upsilon - \frac{\upsilon^2}{2} - \frac{\bar{\alpha}}{2}$$

$$+ C_A\left[\left(\bar{C}_A - \bar{C}_m\right)\tau + \Delta H\right] + \frac{4\sigma P^6}{m^7 R_m^4}\int_o^Y \tilde{K}_p\,\tau^4\,dY \qquad \text{(B-16)}$$

where the dimensionless absorption coefficient is given by:

$$\tilde{K}_p = \frac{K_p L_\mu^*}{\tau^{*1/2}} \qquad \text{(B-17)}$$

# SCHEMATIC REPRESENTATION OF HYPERSONIC SHOCK LAYER

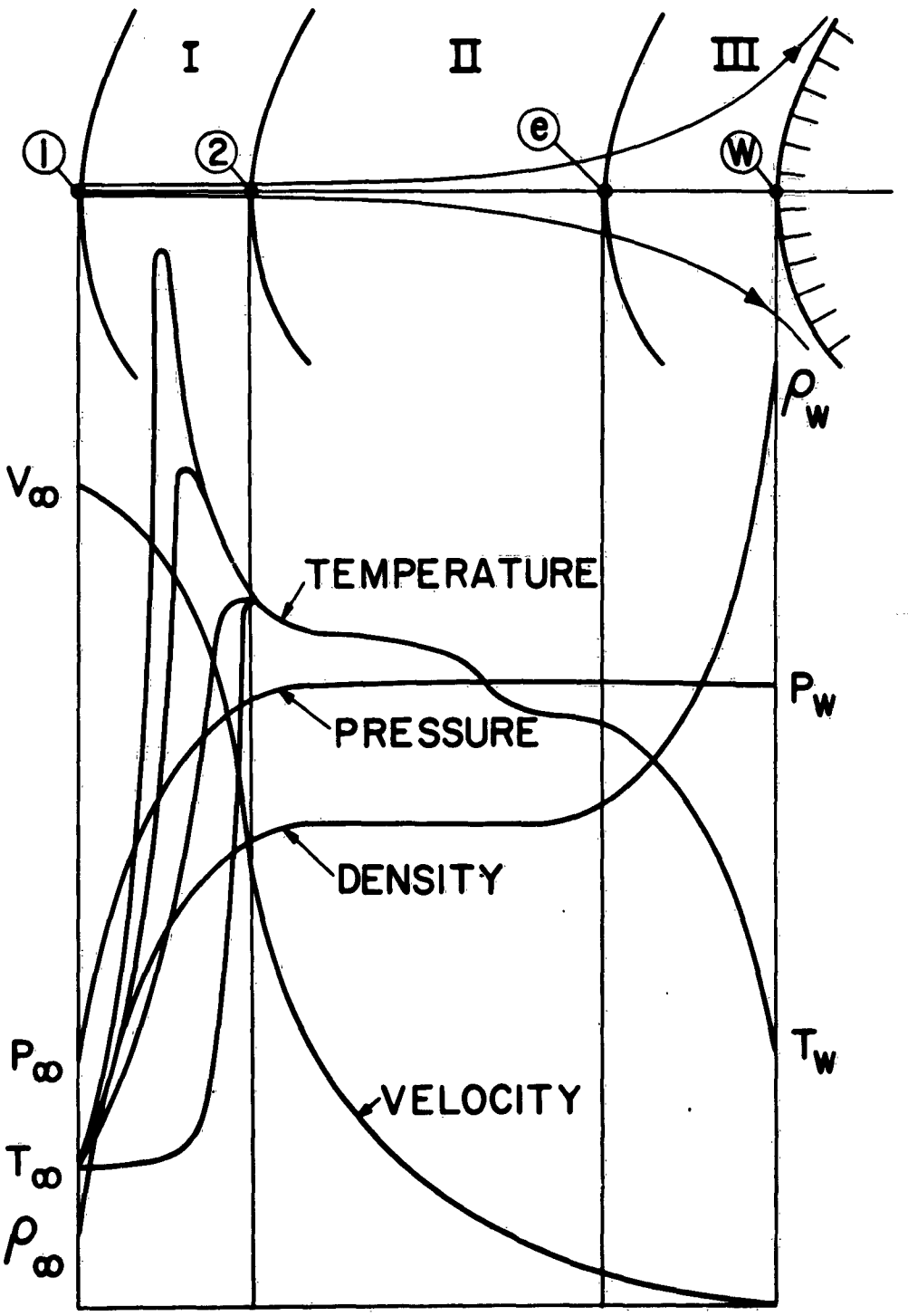


FIGURE 1

VARIATION OF ABSORPTION COEFFICIENT WITH TEMPERATURE AND PRESSURE (LINEARIZED MODEL)

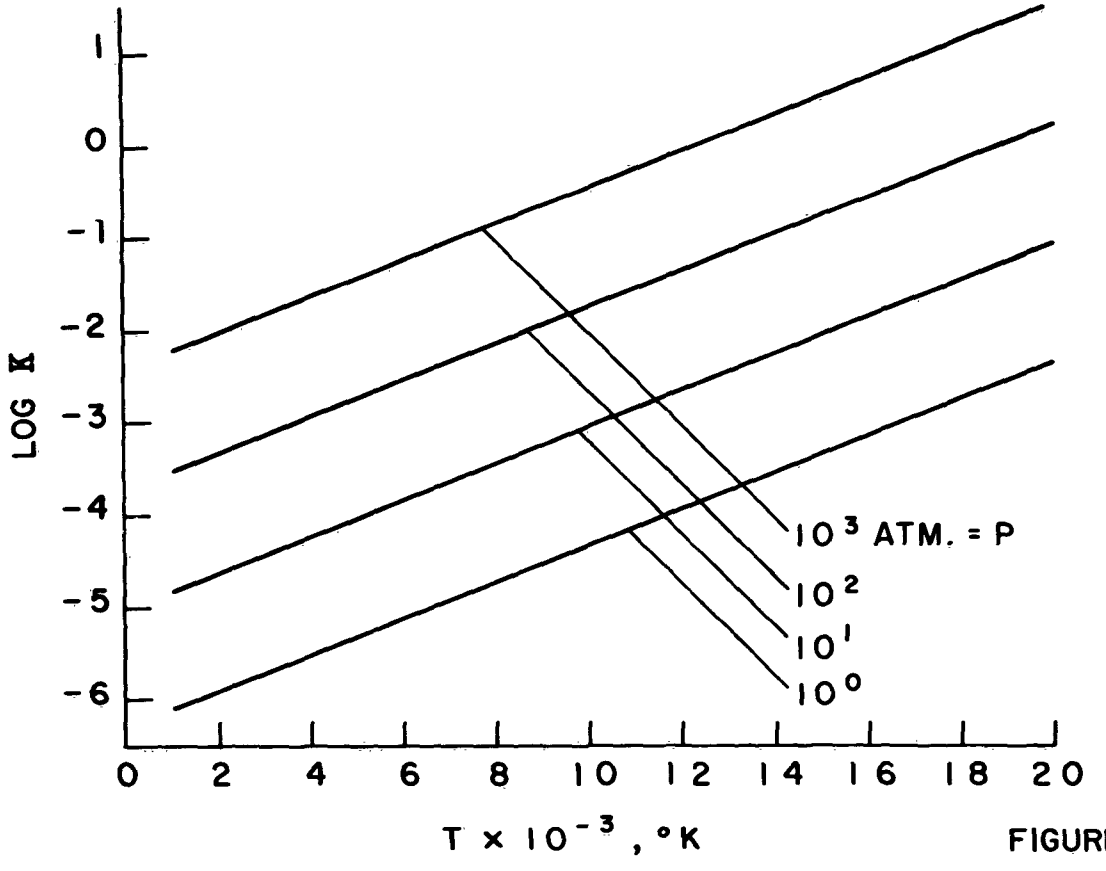


FIGURE 2

VARIATION OF ABSORPTION COEFFICIENT
WITH TEMPERATURE AND PRESSURE

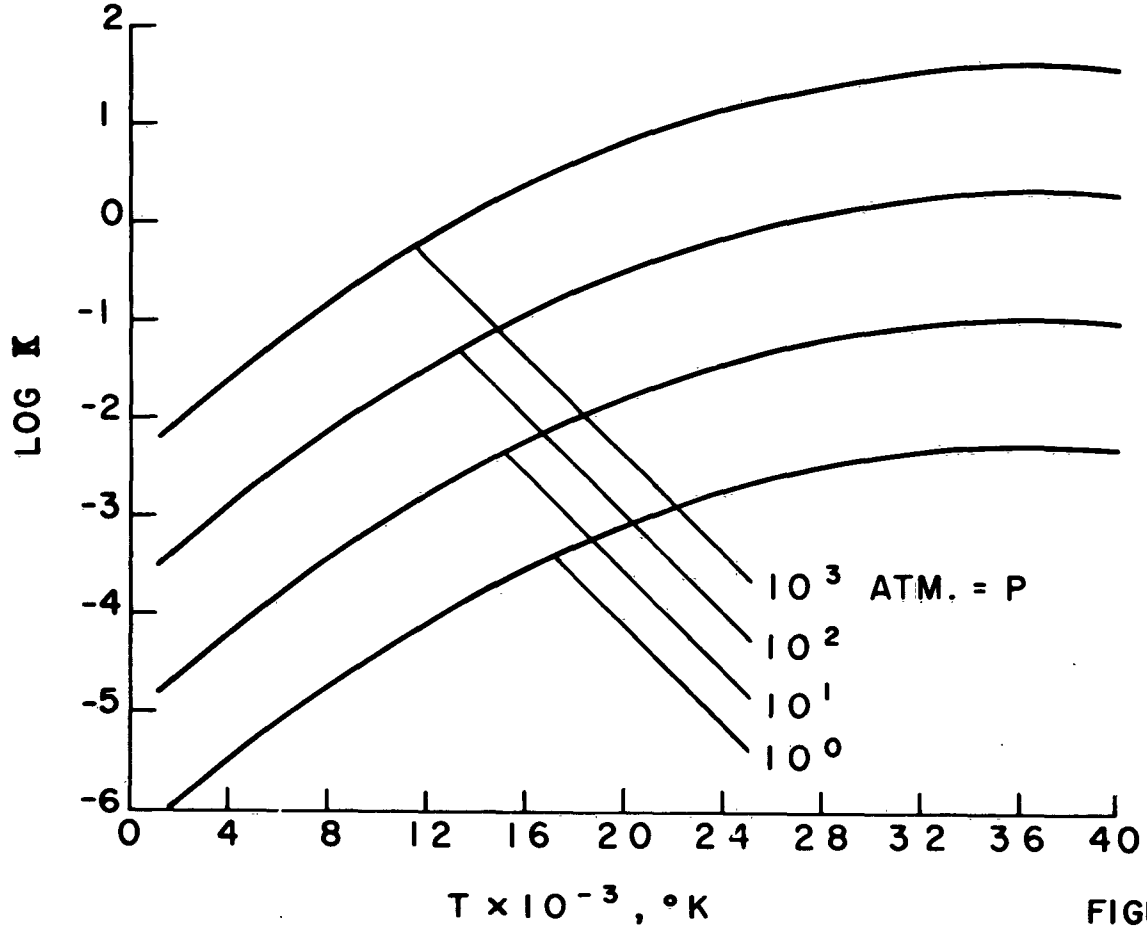


FIGURE 3

# SHOCK WAVE STRUCTURE IN AN OPTICALLY THICK RADIATING GAS, M=12.5

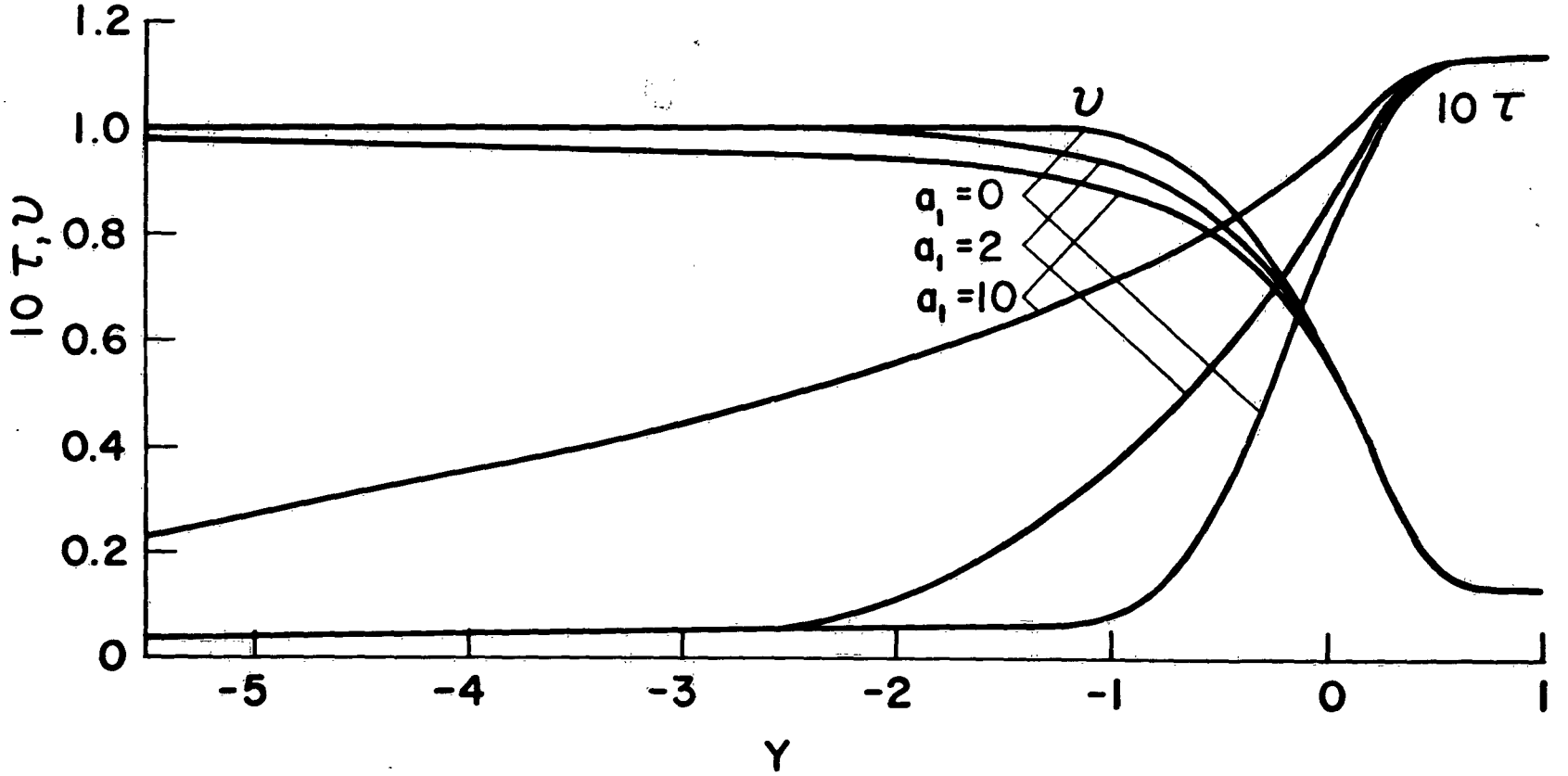


FIGURE 4

# SHOCK WAVE STRUCTURE IN AN OPTICALLY THICK RADIATING GAS, M = 25

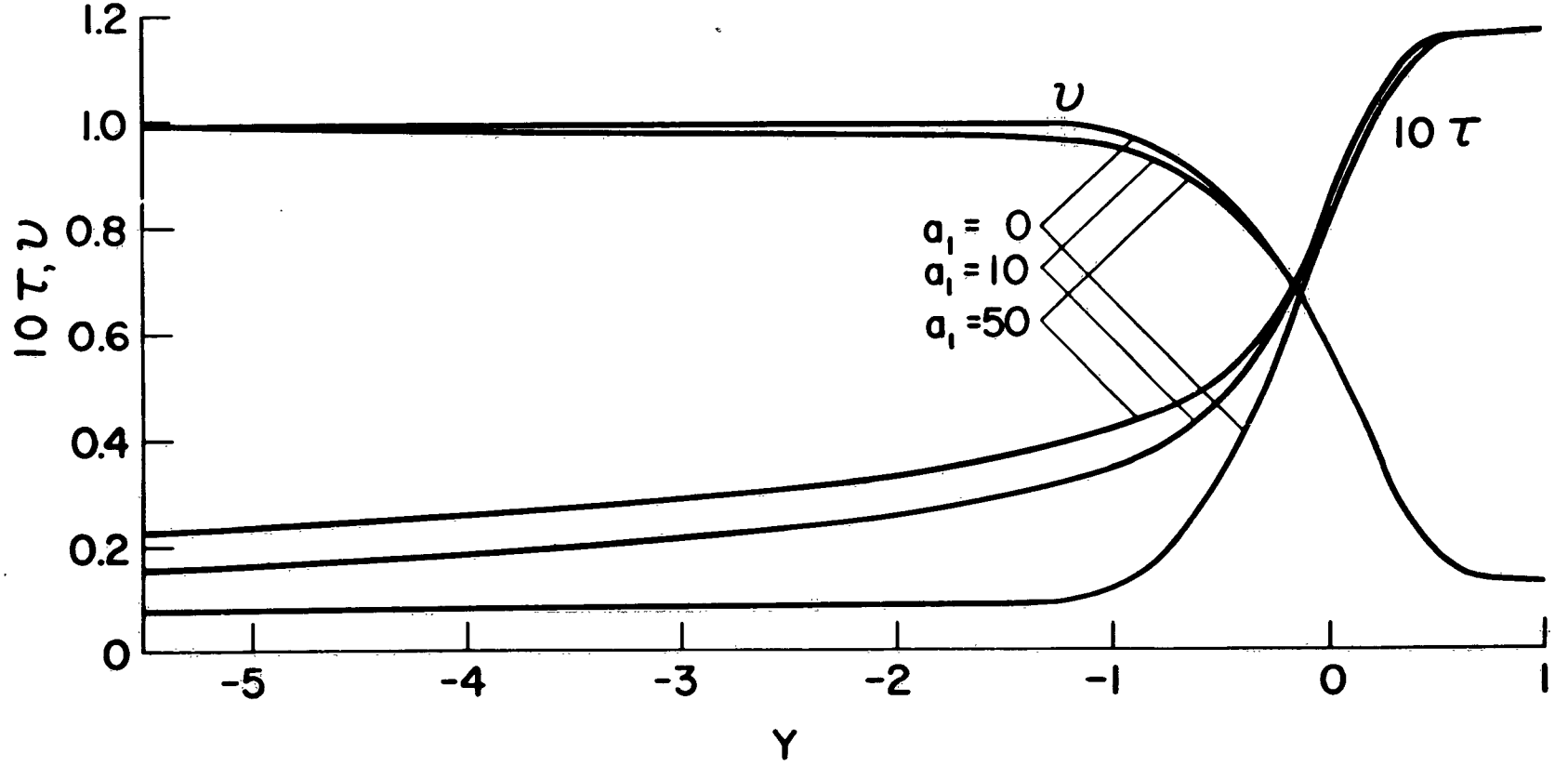


FIGURE 5

# SHOCK WAVE STRUCTURE IN AN OPTICALLY THICK RADIATING GAS, M = 50

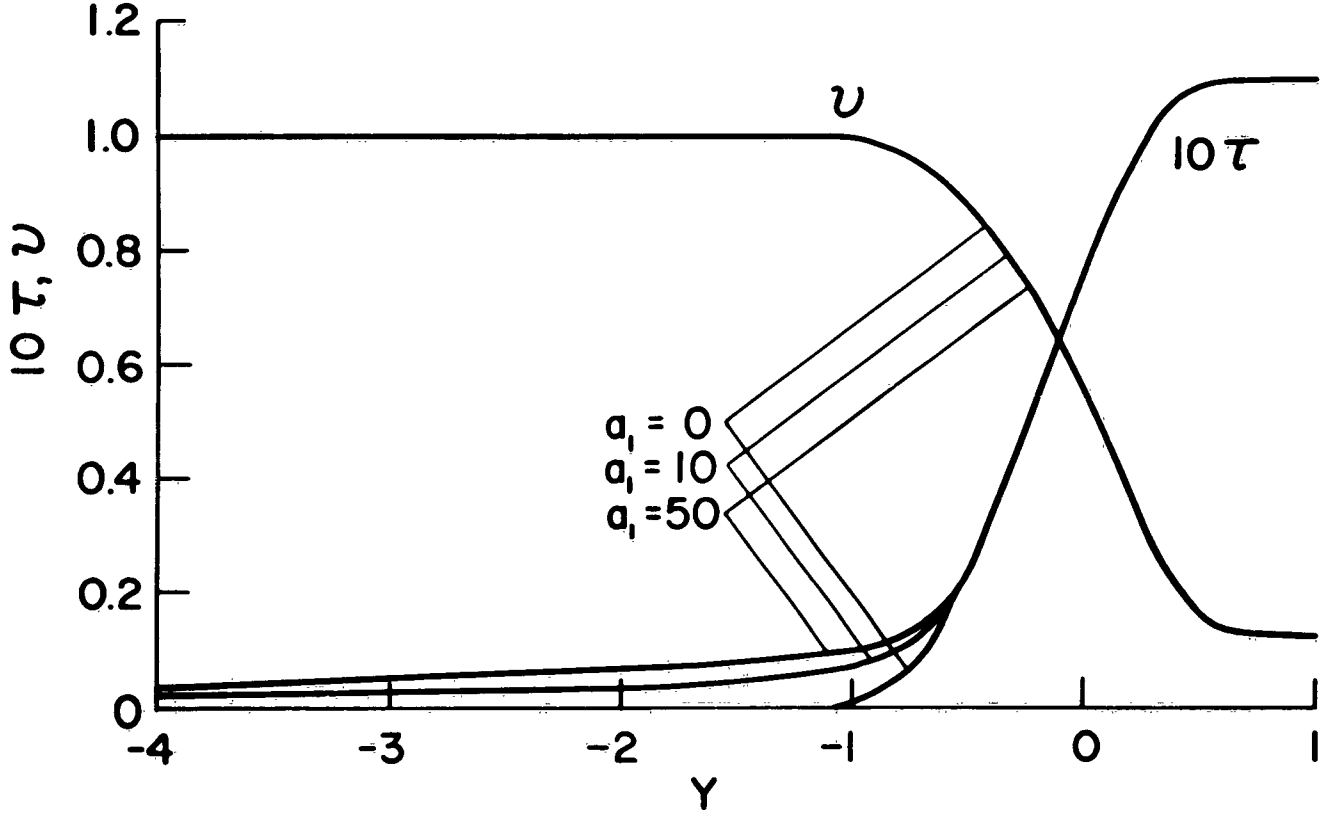


FIGURE 6

DEPENDENCE OF NOMINAL SHOCK WAVE THICKNESS ON RADIATIVE TRANSPORT AND MACH NUMBER

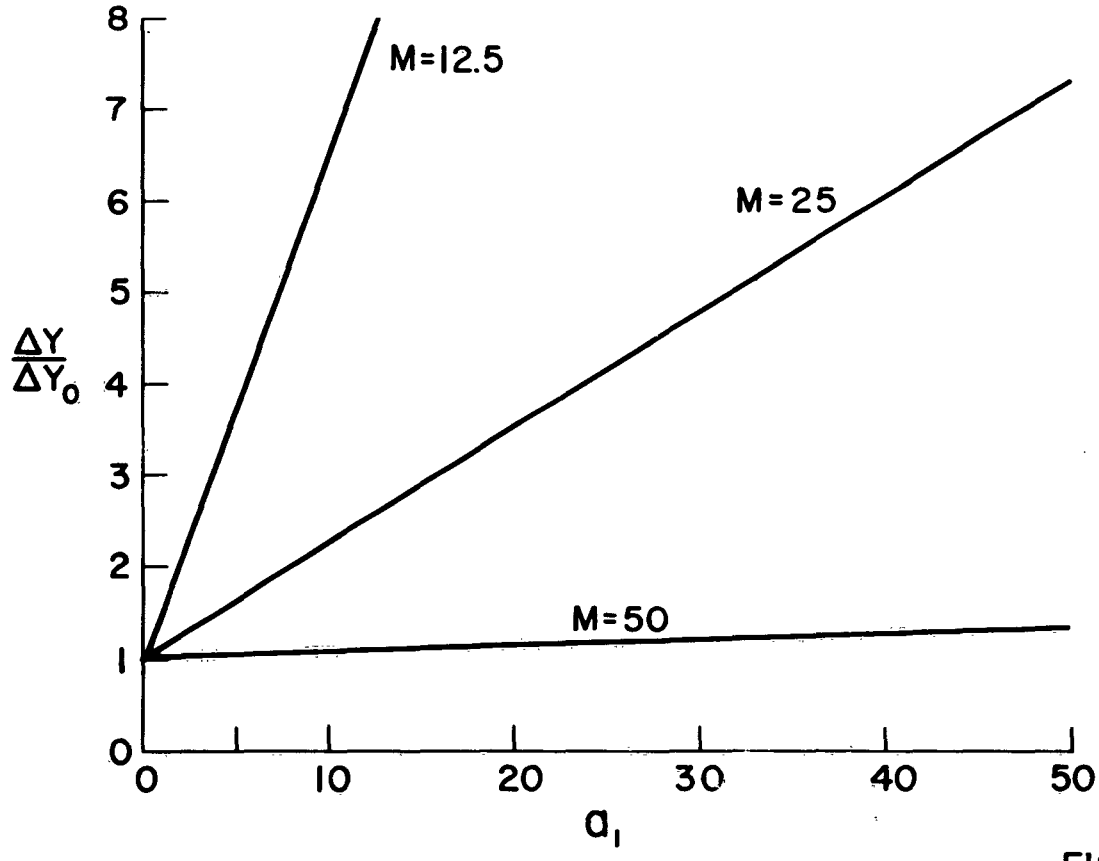


FIGURE 7

# SHOCK WAVE STRUCTURE IN AN OPTICALLY THIN RADIATING GAS, M = 25

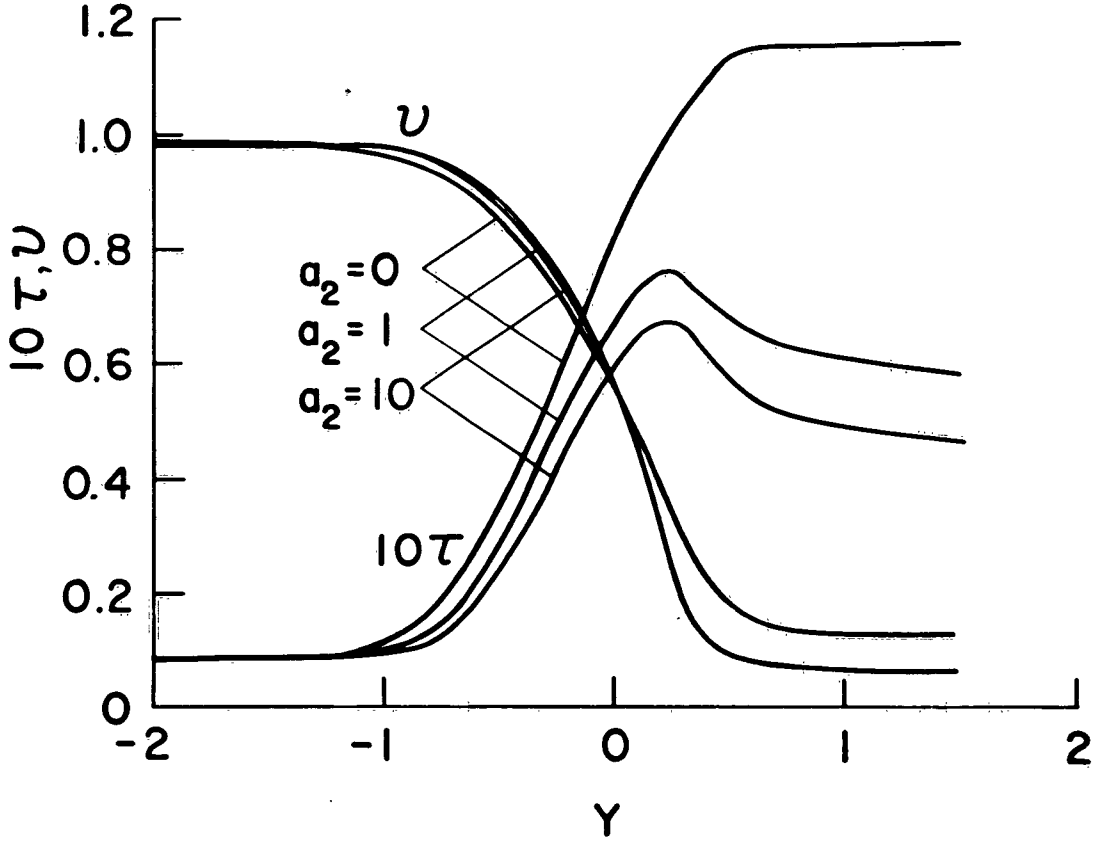


FIGURE 8

# SHOCK WAVE STRUCTURE IN AN OPTICALLY THIN RADIATING GAS WITH DISSOCIATION, M = 25

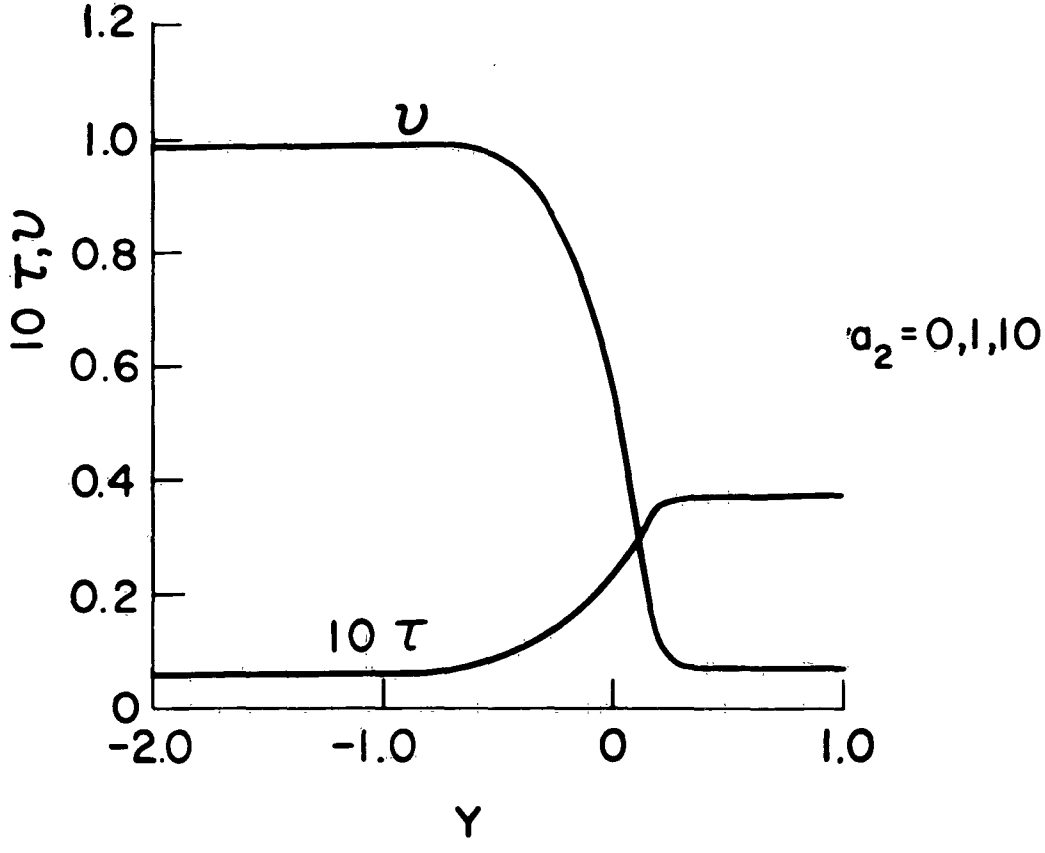


FIGURE 9

# SHOCK WAVE STRUCTURE IN AN OPTICALLY THIN RADIATING GAS, M=35

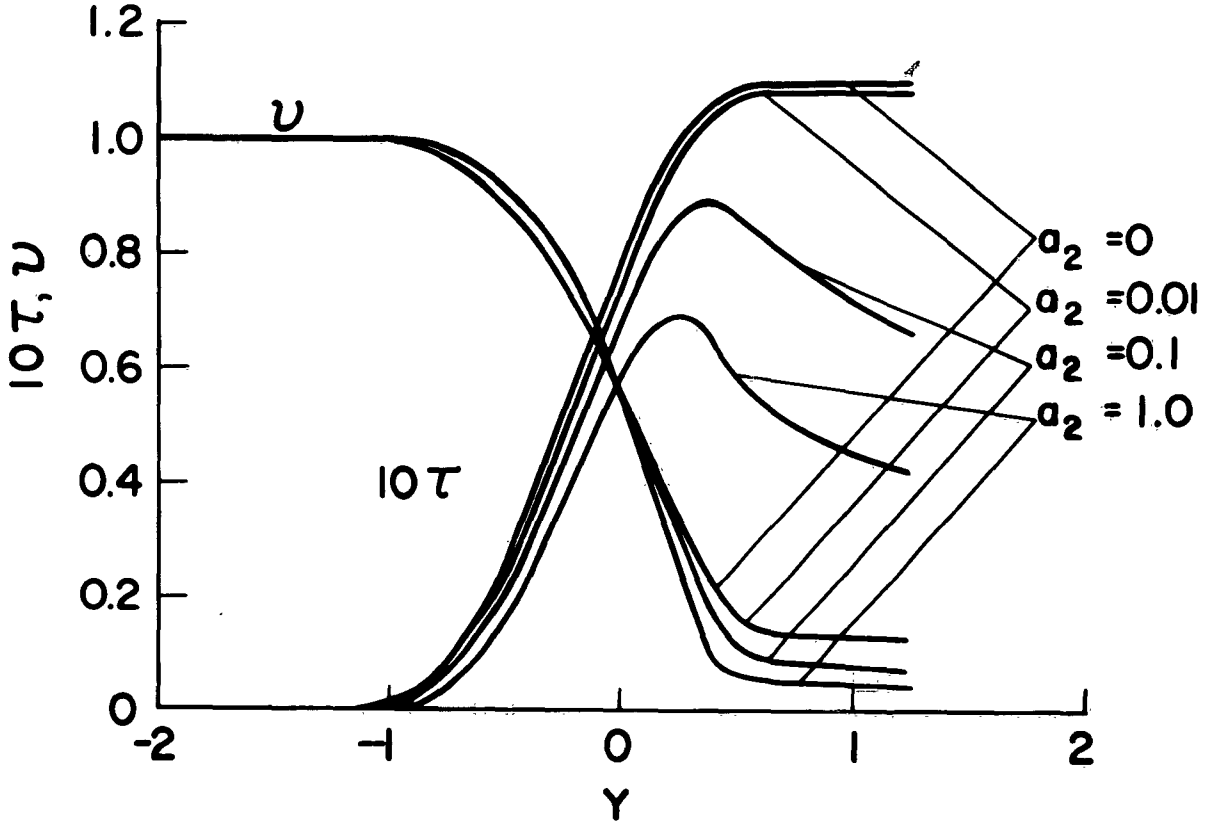


FIGURE 10

# SHOCK WAVE STRUCTURE IN AN OPTICALLY THIN RADIATING GAS WITH DISSOCIATION, M=35

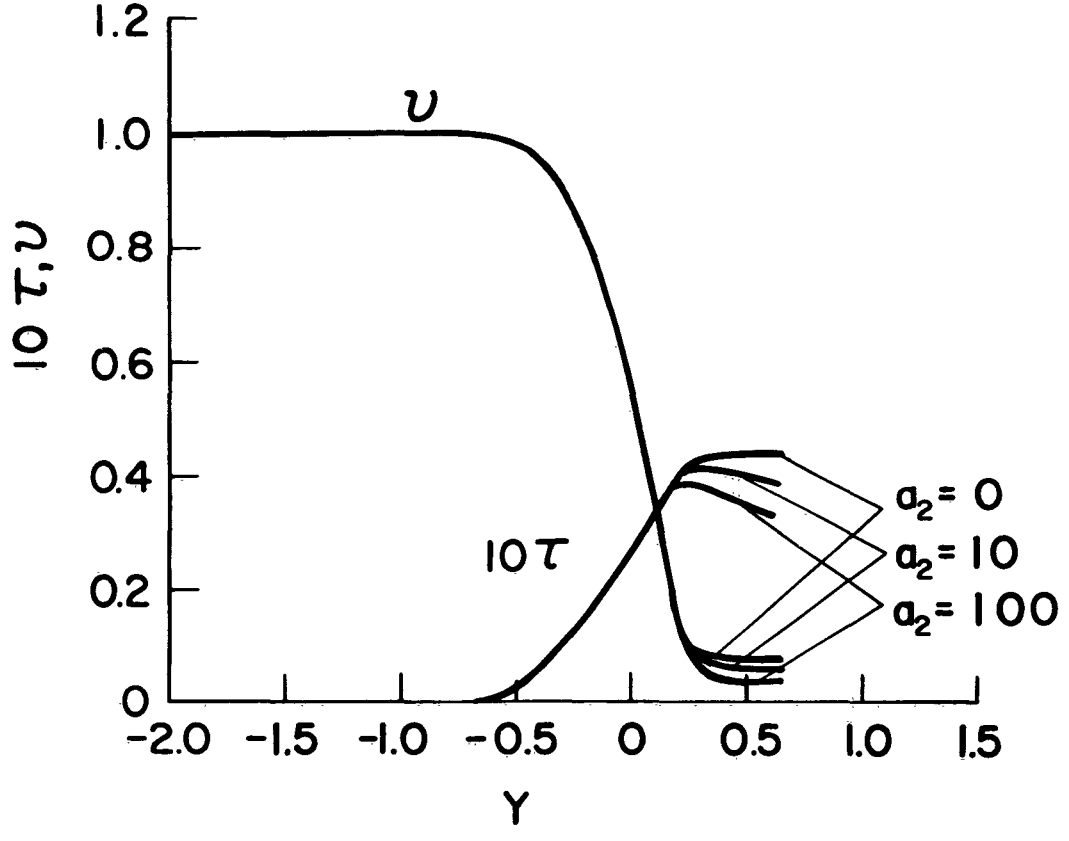


FIGURE 11

# BOUNDARY LAYER STRUCTURE IN AN OPTICALLY THICK RADIATING GAS, (CONSTANT PROPERTIES), $T_e = 20{,}000°R$

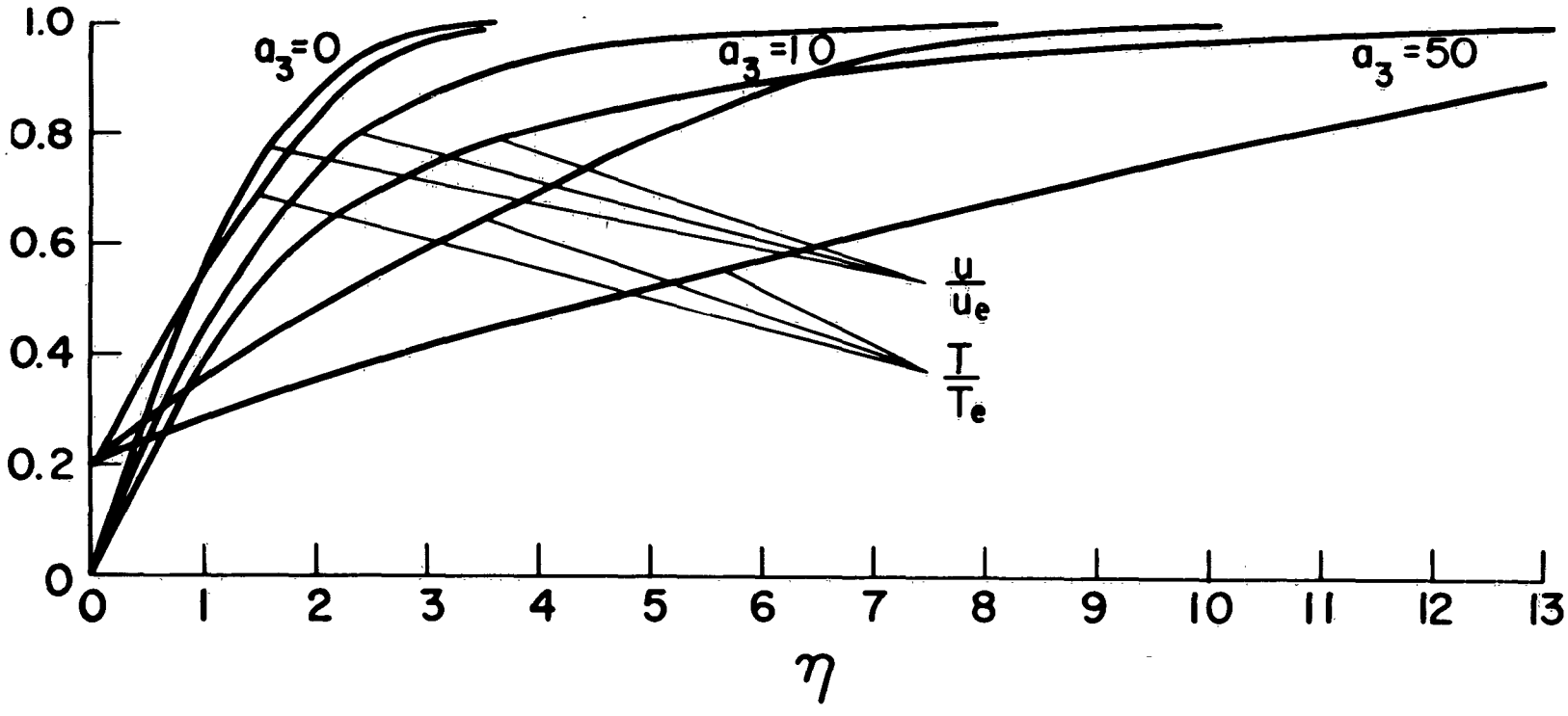


FIGURE 12

BOUNDARY LAYER STRUCTURE IN AN OPTICALLY THICK RADIATING GAS, (CONSTANT PROPERTIES), $T_e = 40{,}000°R$

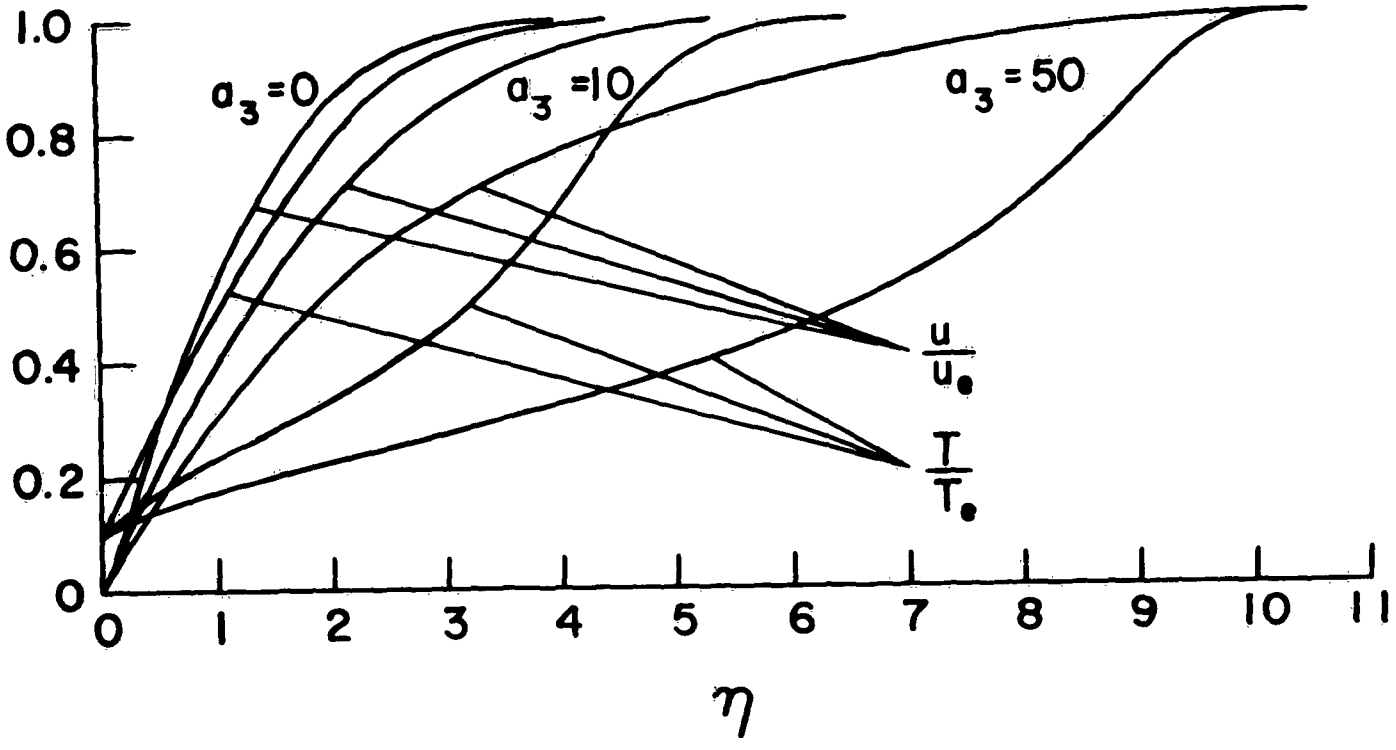


FIGURE 13

BOUNDARY LAYER STRUCTURE IN AN OPTICALLY THICK RADIATING GAS, (VARIABLE PROPERTIES), $T_e = 20{,}000°R$

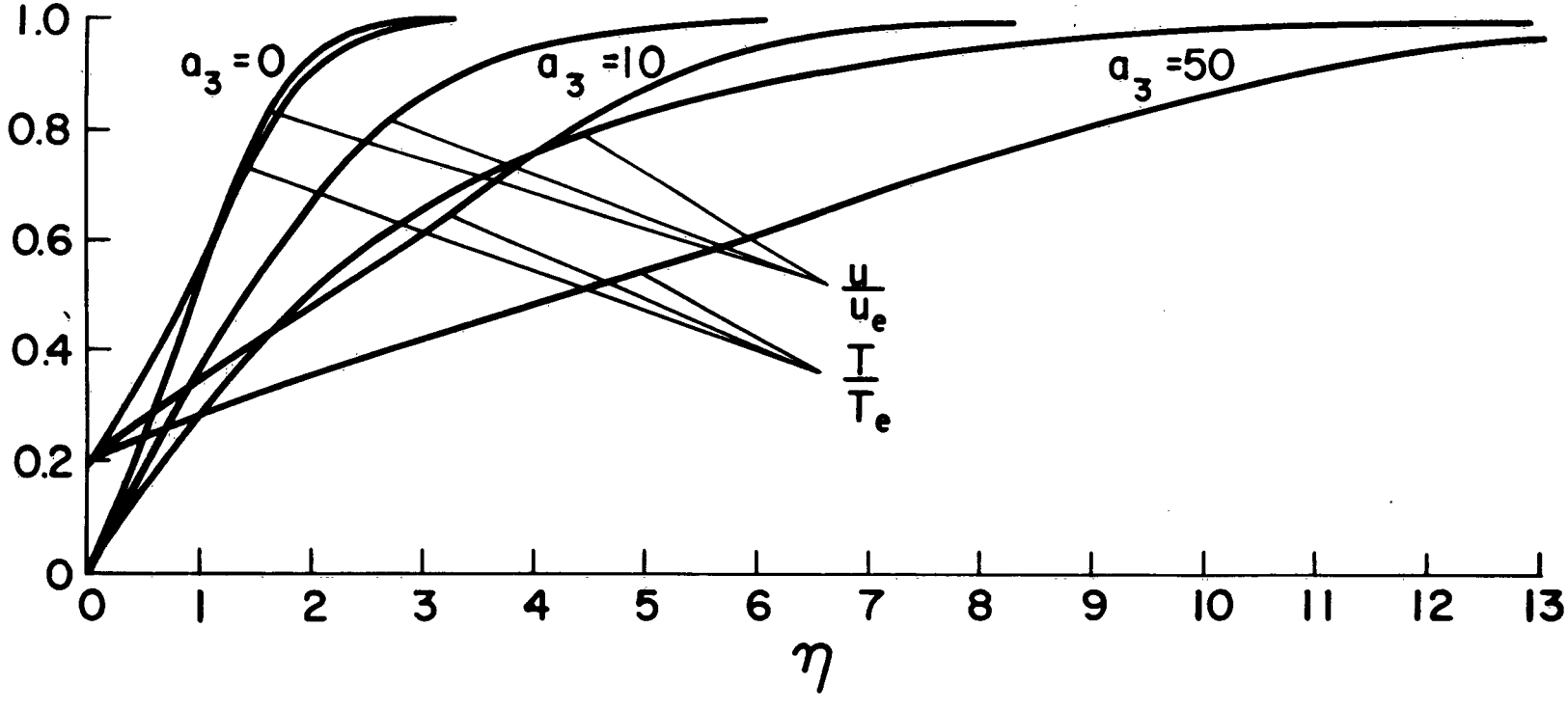


FIGURE 14

BOUNDARY LAYER STRUCTURE IN AN OPTICALLY THICK RADIATING GAS, (VARIABLE PROPERTIES), $T_e = 40{,}000°R$

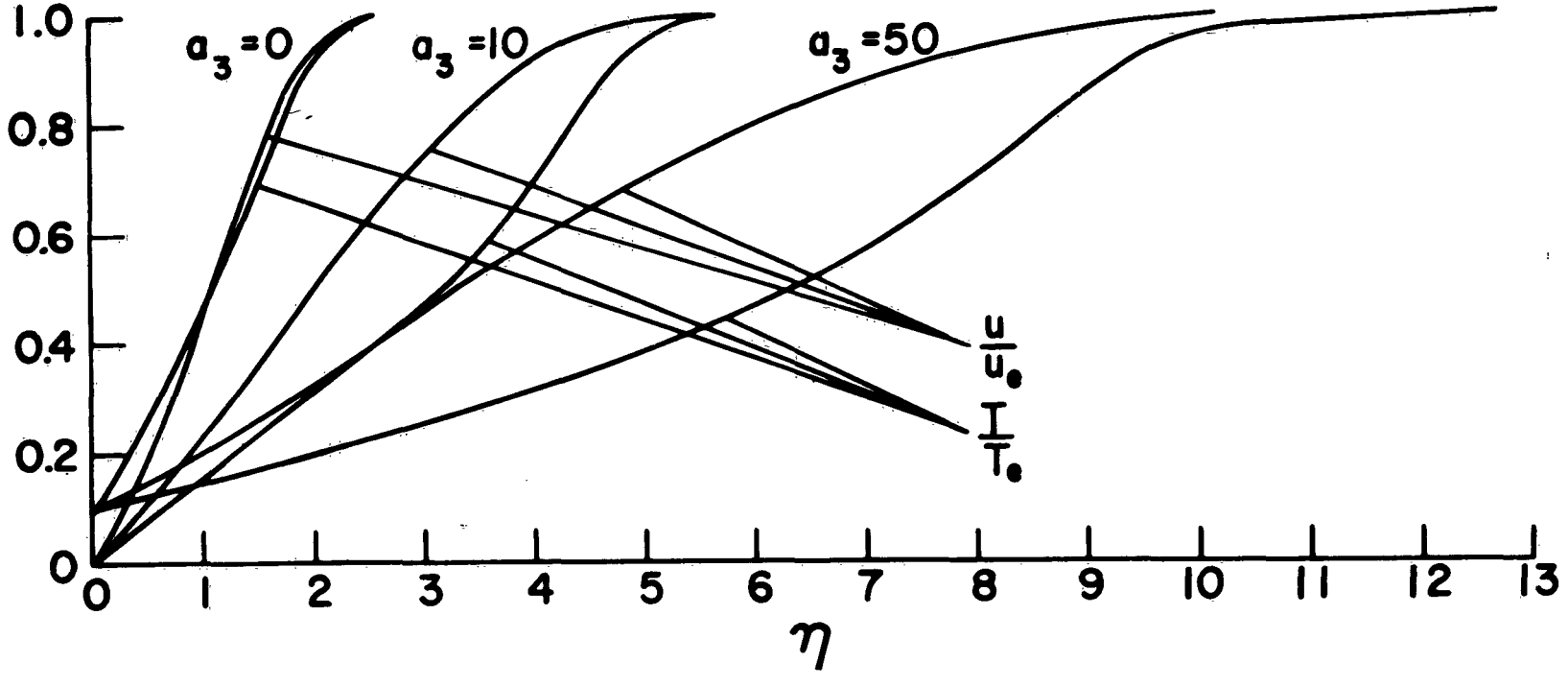


FIGURE 15

# NORMALIZED RADIATIVE PLUS CONDUCTIVE HEAT TRANSFER

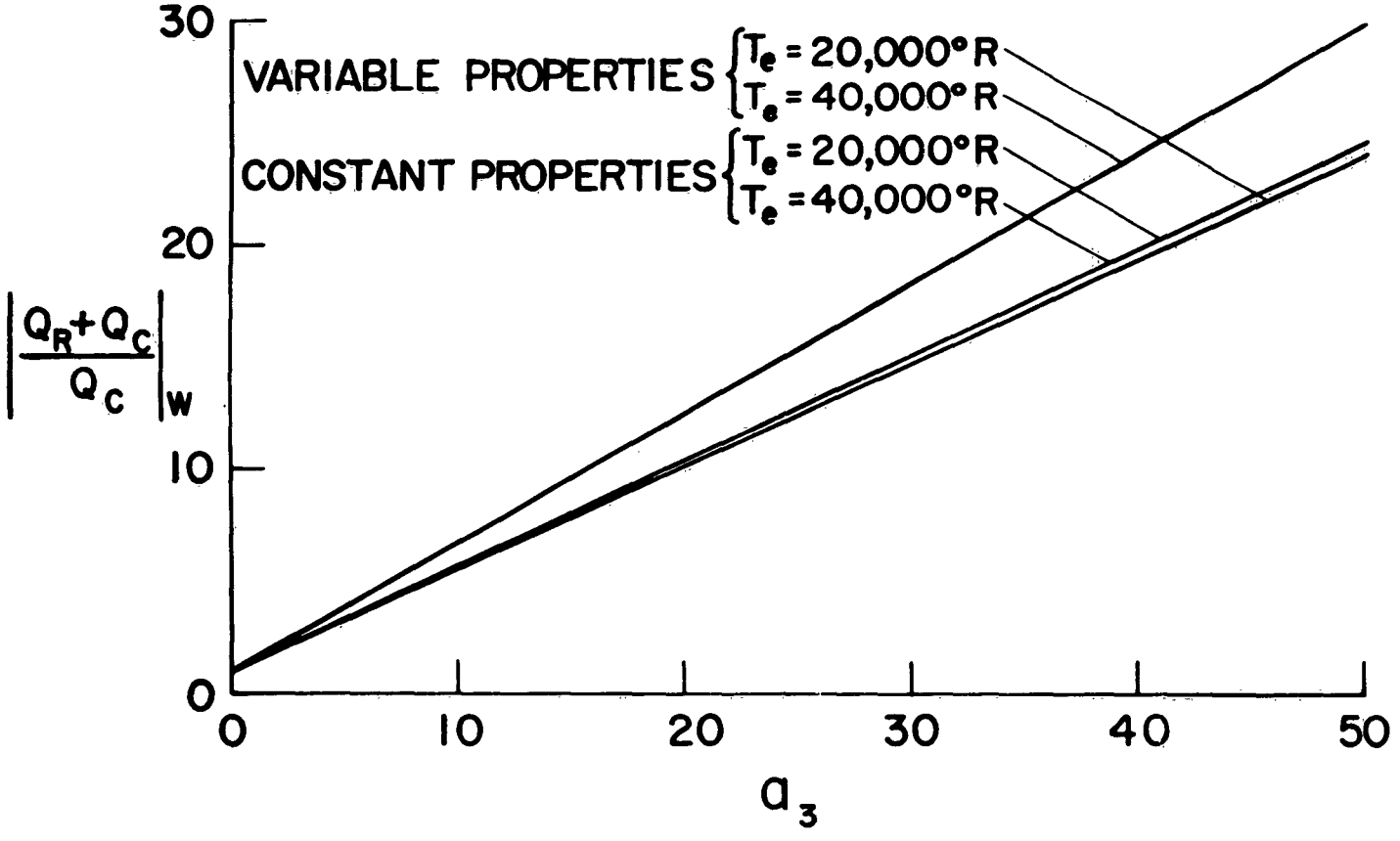


FIGURE 16

VARIATION OF VELOCITY THROUGH A RADIATING OPTICALLY THIN BOUNDARY LAYER, $T_e = 20{,}000\,°R$

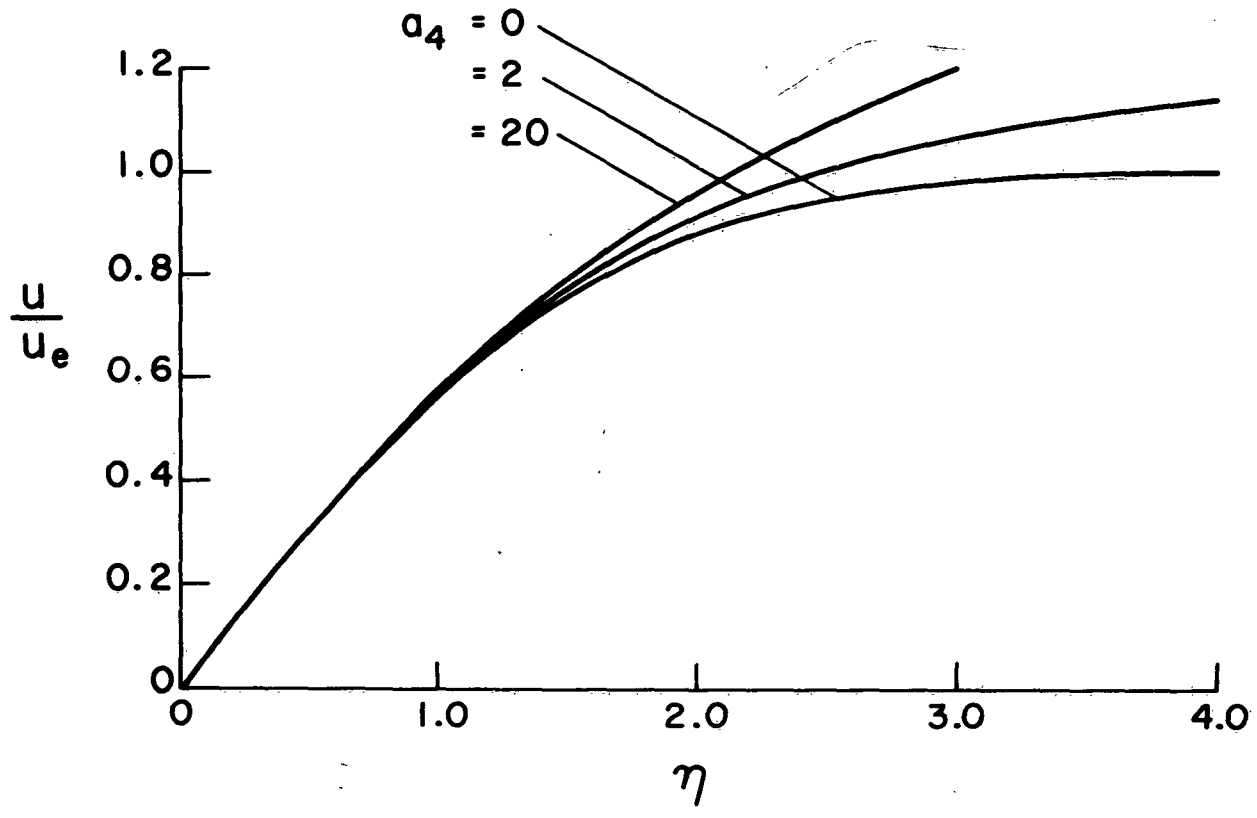


Figure 17

# VARIATION OF TEMPERATURE THROUGH A RADIATING OPTICALLY THIN BOUNDARY LAYER, $T_e = 20{,}000°R$

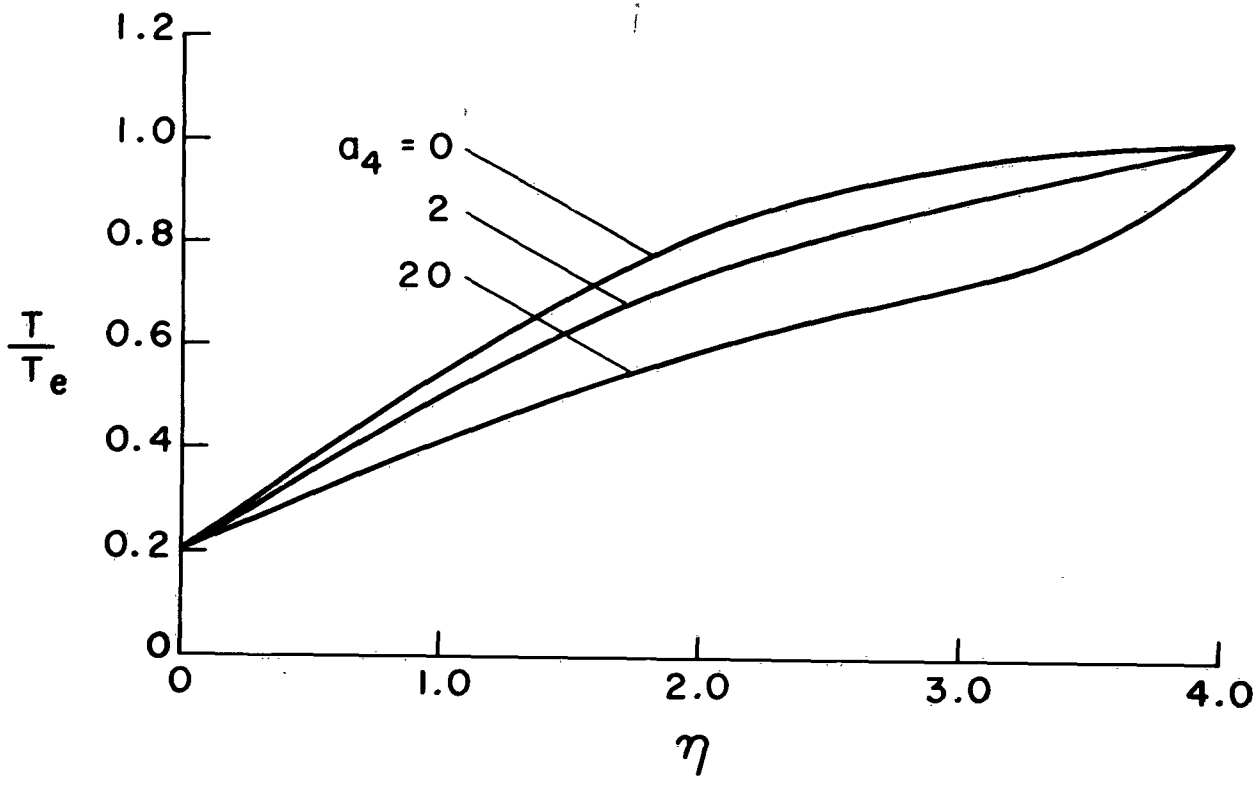


Figure 18

# VARIATION OF RADIATION PARAMETER FOR OPTICALLY THICK GAS

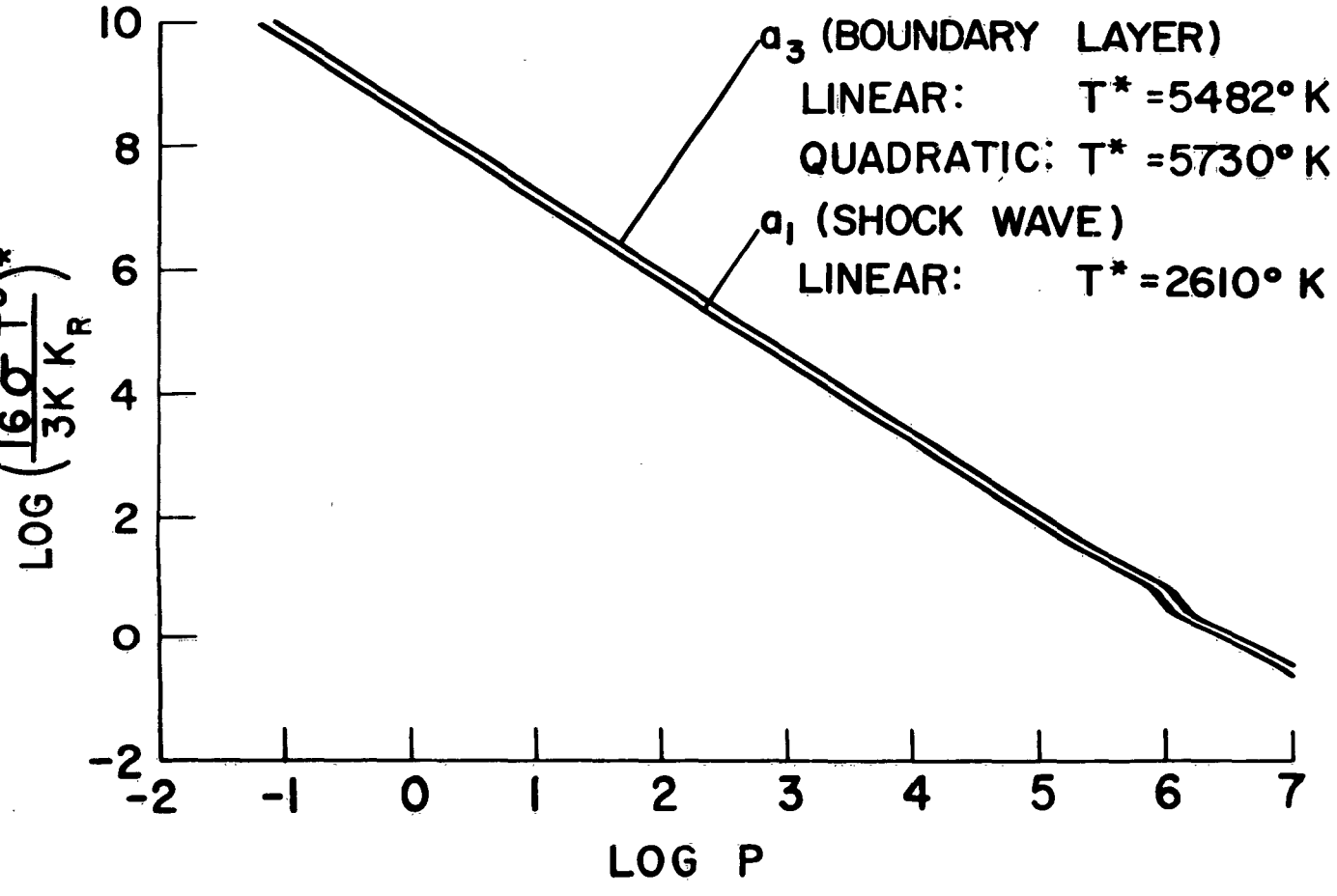


FIGURE 19

GENERAL ELECTRIC

SPACE SCIENCES LABORATORY
MISSILE AND SPACE DIVISION

## TECHNICAL INFORMATION SERIES

| AUTHOR | SUBJECT CLASSIFICATION | NO. |
|---|---|---|
| S. M. Scala<br>D. H. Sampson | Radiation, Hypersonic Flow | R63SD46 |
| | | DATE<br>March 1963 |
| TITLE<br>HEAT TRANSFER IN HYPERSONIC FLOW WITH RADIATION AND CHEMICAL REACTION | | G. E. CLASS<br>I |
| | | GOV. CLASS<br>Unclassified |
| REPRODUCIBLE COPY FILED AT MSD LIBRARY, DOCUMENTS LIBRARY UNIT, VALLEY FORGE SPACE TECHNOLOGY CENTER, KING OF PRUSSIA, PA. | | NO. PAGES<br>78 |


SUMMARY

The effect of radiative transport on the structure of the shock layer produced in front of a hypersonic vehicle in an earth-like atmosphere is studied. Specifically, the effects of radiation on the structure of the boundary layer and the shock wave are determined numerically for the optically thick and optically thin limits.

In the optically thin limit, the effect of radiation is to reduce the peak shock temperature. Also, on the downstream side, the temperature continues to decay with distance because the gas continues to emit, and the solution must be matched to that pertaining to the contiguous inner viscous layer. On the other hand, the peak shock temperature and the Rankine-Hugoniot conditions are unaffected by the radiation in the optically thick limit, but both boundary layer and shock wave are broadened by the radiation. Although it is found that the boundary layer and shock wave are actually never optically thick, neither are they always optically thin. Thus, some of the radiation emitted is reabsorbed in the boundary layer and shock wave and they are thereby "radiation" broadened to some degree. The broadening is expected to be largest for high temperatures and when the total shock layer is optically thick or nearly so. It is also pointed out that the gray gas approximation is very poor for high temperature air.


By cutting out this rectangle and folding on the center line, the above information can be fitted into a standard card file.


AUTHOR S. M. Scala S. M. Scala D. H. Sampson D. H. Sampson

COUNTERSIGNED Joseph Farber Joseph Farber